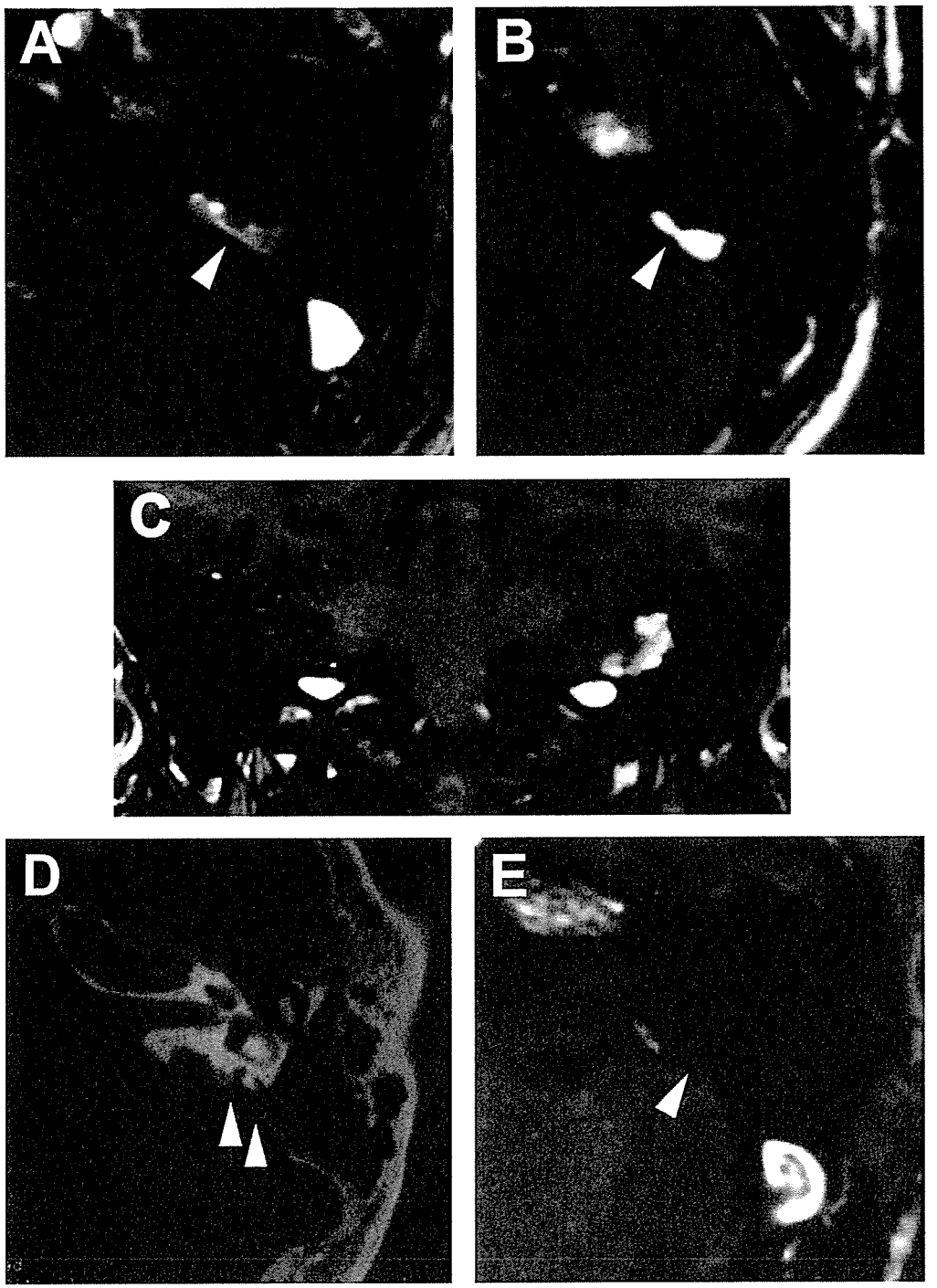

Fig. 2. Magnetic resonance (MR) and computed tomography (CT) images of the tumor. Axial T1-weighted (A) and T2-weighted with FLAIR (B) MRIs reveal a hyperintense cholesterol granuloma (CG) (arrowheads) adjacent to the endolymphatic sac. (C) Coronal T1-weighted MRI shows the CG (arrowhead) with heterogeneous signal intensity. (D) Axial CT shows the CG (arrowheads) abutting the endolymphatic sac. (E) Axial T2-weighted MRI taken 6 months after surgical resection of the CG mass. Recurrence of the CG is not apparent (arrowhead indicates the part surrounding ES).

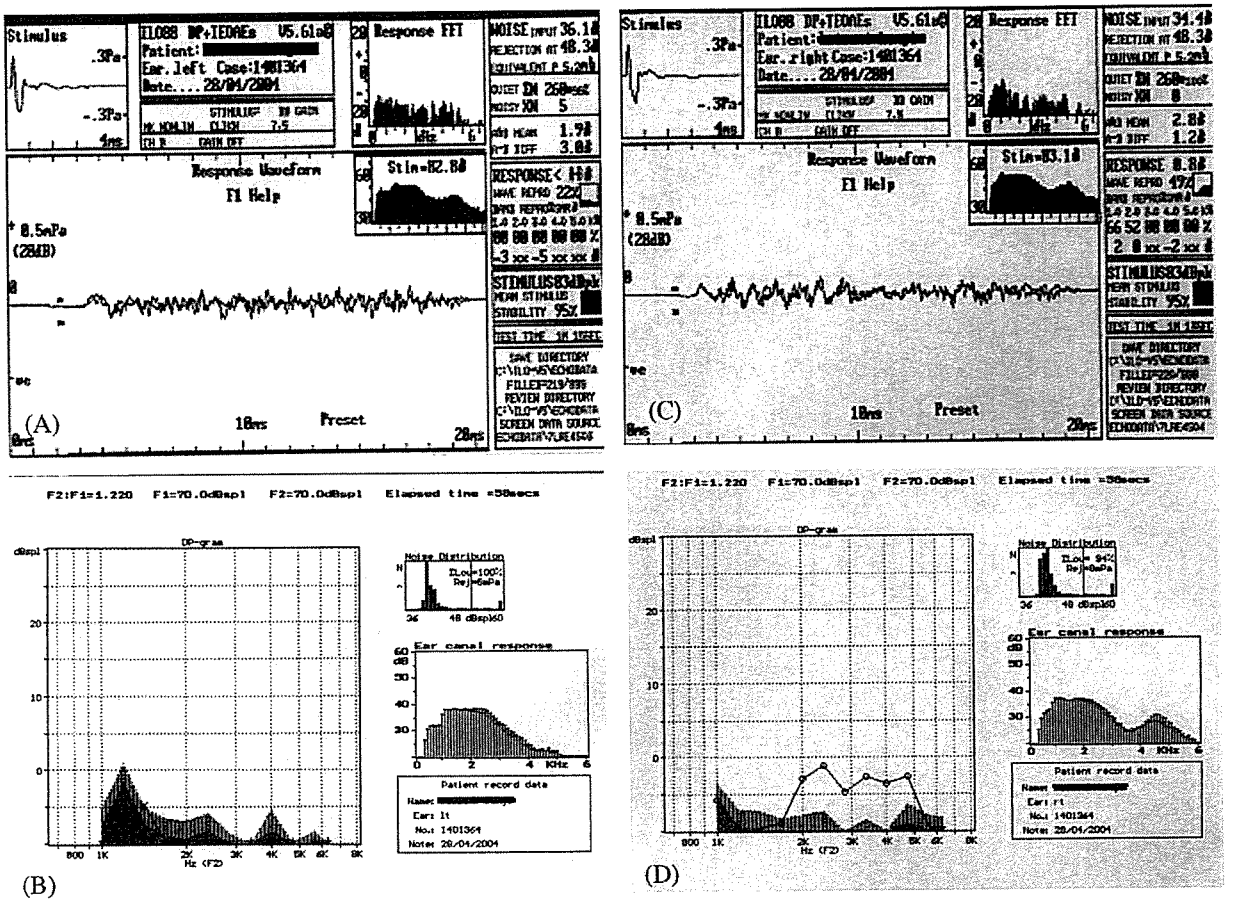

Fig. 3. Transient-evoked otoacoustic emission (TEOAE) and distorted product otoacoustic emission (DPOAE) measurements. (A and B) TEOAE. (C and D) DPOAE. Left ear (A and C) and right ear (B and D). There were no TEOAE and DPOAE responses from the left ear.

3. Discussion

This patient displayed symptoms characteristic of Meniere's disease, but had a CG surrounding the ES. The tumor surrounding ES is typically considered as ELST. CGs surrounding ES, as the one described in our case, is very rare. Although CGs can be generated anywhere in the temporal bone, CGs affecting anterior parts of the petrous apex occur typically [1].

The point of this case was differential diagnosis to distinguish CG from ELST at the pre-operation. In MRI, CGs typically exhibit high signal on T1- and T2-weighted images resulting from the paramagnetic effect of hemoglobin [3,4]. However, ELST lesions characteristically appear heterogeneous with scattered areas of signal and peripheral rim enhancement on T1-weighted images [5]. During the operation, we found fluid in the mastoid cells around the ES. We finally diagnosed the tumor as a CG because its histopathology revealed the presence of cholesterol crystals and several hemosiderin-containing macrophages but no papillary adenoma or adenocarcinoma. In addition, tumor demonstrated no S-100 specific staining which is one of the ELST markers [5] or neurogenic tumor.

Additionally, ELST includes sporadic ELST and ELST associated with von Hippel-Lindau (VHL) disease which is an autosomal dominant multisystem disorder [6]. Thus far, our patient remains free of such complications.

The etiology of this CG is unknown. There are two theories of etiology including classic and new theories. We speculated that the CG in this patient formed according to the classic theory of CG formation. That is, because the air cells within the petrous apex are convoluted and deeply embedded, they are difficult to aerate and drain in decreased atmospheric pressure, thus causing mastoid cells to hemorrhage. The subsequent catabolism of hemoglobin or breakdown of local tissues generates cholesterol, which in turn produces a "foreign body" or cell-mediated immune response [7–10]. On the other hand, a new theory proposed by Jackler and Cho demonstrated that CGs of the anterior petrous apex may arise from proclivous bone marrow and mucosa that ruptures, causing blood to pool within the anterior petrous apex [1]. However, this CG was not located in anterior petrous apex. This etiology may be different from new theory.

Hansen and Luxford described the surgical resections of 13 ELSTs and in their series one patient who had undergone transmastoid surgery for the resection of a presumed CG had

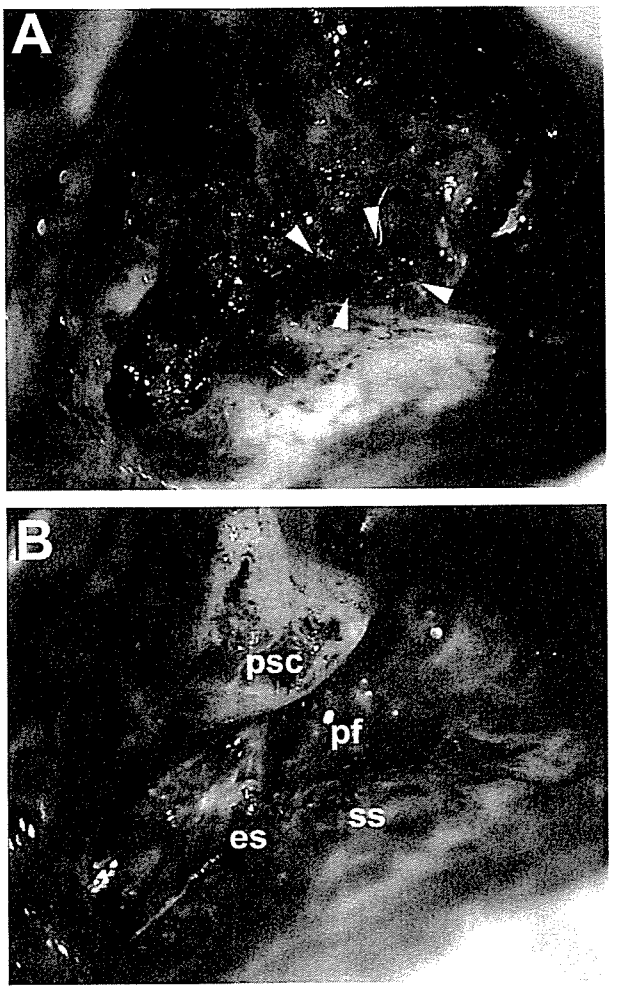

Fig. 4. Photograph of the operative field. (A) Arrowheads indicate wall of the cholesterol granuloma (CG). (B) Mastoid and endolymphatic sac after aspiration. *Abbreviations*: es, endolymphatic sac; psc, posterior semicircular canal; lsc, lateral semicircular canal; ss, sigmoid sinus; ps, posterior fossa.

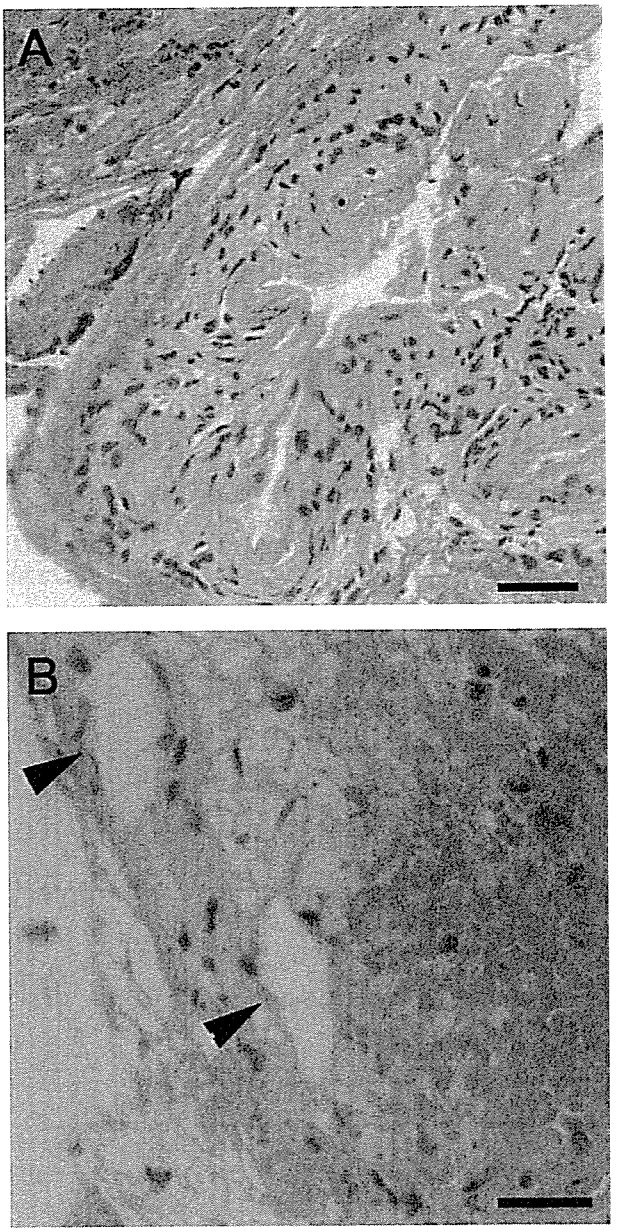

Fig. 5. Low (A) and high (B) magnification photomicrographs of a section through the excised cholesterol granuloma (CG) showing its histopathology. The CG mainly consisted of granulation tissue. A few cholesterol crystals (arrowheads) were also found. Scale bars: (A) 50 μm and (B) 15 μm.

a recurrence of the ELST 2 years after the initial operation [2]. This case might be also secondary CG followed by hemorrhage of small ELST although histological study has demonstrated granulation tissue so far. We need follow-up this case to detect the recurrence of tumor and occurrence of ELST. Therefore, a long-term follow-up (>24 months postoperative) of these patients is needed although MRI has not revealed the presence of ELSTs up to 12 months after surgery.

We discuss the correlation between the CG and Meniere's syndrome. Before the operation, the patient demonstrated negative in the glycerol test, which is often performed in suspected cases of Meniere's syndrome or hydrops. In humans, the ES of the inner ear have been suggested to control endolymph volume and homeostasis [11,12]. In most patients with endolymphatic hydrops, glycerol intake typically reduces endolymphatic fluid, but in our patient, endolymphatic fluid pressure remained unchanged because the CG supplied continuous pressure onto the ES. We speculated that the CG-associated pressure onto the ES induced the Meniere's syndrome-like symptoms in this patient. Because of these symptoms, it was difficult to determine preoperatively whether this pathology was hydrops. Indeed, it is often difficult to distinguish Meniere's syndrome from ELSTs on the sole basis of preoperative symptoms. Hansen and Luxford recently reported that only 3 of 14 ELST patients they examined actually had Meniere's syndrome [2]. ELSTs develop and press ES, inducing progressive hearing loss and repeated vertigo attacks [2]. Therefore, we speculated that CG in this case might develop after hemorrhage, pressed ES and then patients presented progressive symptoms.

Identification of small or in situ ELSTs offers patients to opt for the surgical removal of the tumors with the aim of hearing preservation [13]. Although we made a special effort to keep the ES intact during surgery, audiogram performed 2 months after surgery revealed that the patient's level of hearing was worse than preoperative levels. However, audiogram performed 12 months after surgery revealed that the patient's hearing has steadily improved but not to preoperative levels. In the present case, the patient's OAE response to stimuli was poor, thus, prompting us to speculate a poor prognosis for this patient in terms of postoperative recovery of hearing function. Additionally, the oscilation of drilling bone might result in ES, although ES macroscopically appeared intact.

In conclusion, we report the very rare case of a CG surrounding the ES. MRI was very useful for diagnosis. OAEs revealed the left-sided cochlear damage. Surgery was successful in draining the brown fluid from the CG mass. Vertigo and headache improved within 6 months after operation. Hearing function has recovered to some extent but not completely.

References

[1] Jackler RK, Cho M. A new theory to explain the genesis of petrous apex cholesterol granuloma. Otol Neurotol 2003;24:96–106.

[2] Hansen MR, Luxford WM. Surgical outcomes in patients with endolymphatic sac tumors. Laryngoscope 2004;114:1470–4.

[3] Chang P, Fagan PA, Atlas MD, Roche J. Imaging destructive lesions of the petrous apex. Laryngoscope 1998;108:599–604.

[4] Kosling S, Bootz F. CT and MR imaging after middle ear surgery. Eur J Radiol 2001;40:113–8.

[5] Devaney KO, Ferlito A, Rinaldo A. Endolymphatic sac tumor (low-grade papillary adenocarcinoma) of the temporal bone. Acta Otolaryngol 2003;123:1022–6.

[6] Lonser RR, Kim HJ, Butman JA, Vortmeyer AO, Choo DI, Oldfield EH. Tumors of the endolymphatic sac in von Hippel-Lindau disease. N Engl J Med 2004;350:2481–6.

[7] Beaumont GD. The effects of exclusion of air from pneumatized bones. J Laryngol Otol 1966;80:236–49.

[8] Friedmann I. Epidermoid cholesteatoma and cholesterol granuloma; experimental and human. Ann Otol Rhinol Laryngol 1959;68:57–79.

[9] Main TS, Shimada T, Lim DJ. Experimental cholesterol granuloma. Arch Otolaryngol 1970;91:356–9.

[10] Goycoolea MV, Paparella MM, Juhn SK, Carpenter AM. Otitis media with perforation of the tympanic membrane: a longitudinal experimental study. Laryngoscope 1980;90:2037–45.

[11] Salt AN. Regulation of endolymphatic fluid volume. Ann N Y Acad Sci 2001;942:306–12.

[12] Couloigner V, Berrebi D, Teixeira M, Paris R, Florentin A, Bozorg Grayeli A, et al. Aquaporin-2 in the human endolymphatic sac. Acta Otolaryngol 2004;124:449–53.

[13] Megerian CA, Haynes DS, Poe DS, Choo DI, Keriakas TJ, Glasscock 3rd ME. Hearing preservation surgery for small endolymphatic sac tumors in patients with von Hippel-Lindau syndrome. Otol Neurotol 2002;23:378–87.

ARTICLE

doi:10.1016/j.ymthe.2005.09.020

Histopathological and Behavioral Improvement of Murine Mucopolysaccharidosis Type VII by Intracerebral Transplantation of Neural Stem Cells

Yasuyuki Fukuhara,[1,2] Xiao-Kang Li,[3] Yusuke Kitazawa,[3] Masumi Inagaki,[4] Kentaro Matsuoka,[5] Motomichi Kosuga,[1] Rika Kosaki,[1,2] Takuya Shimazaki,[6] Hitoshi Endo,[7] Akihiro Umezawa,[8] Hideyuki Okano,[6] Takao Takahashi,[2] and Torayuki Okuyama[1,2,*]

[1]*Department of Clinical Genetics and Molecular Medicine,* [3]*Department of Innovative Surgery,* [8]*Department of Reproductive Biology, and* [5]*Department of Pathology, National Center for Child Health and Development, 2-10-1 Okura, Setagaya-ku, Tokyo 157-8535, Japan*
[2]*Department of Pediatrics and* [6]*Department of Physiology, Keio University School of Medicine, 35 Shinanomachi, Shinjuku-ku, Tokyo 160-8582, Japan*
[4]*National Center of Neurology and Psychiatry, 1-7-1 Kounodai, Ichikawa-shi, Chiba 272-8516, Japan*
[7]*Biochemistry of Experimental Medicine, Jichi Medical School, Minamikawachi-machi, Kawachi-gun, Tochigi 329-0498, Japan*

**To whom correspondence and reprint requests should be addressed. Fax: +81 3 3416 2222. E-mail: okuyama-t@ncchd.go.jp.*

Available online 28 November 2005

The therapeutic efficacy of neural stem cell transplantation for central nervous system (CNS) lesions in lysosomal storage disorders was explored using a murine model of mucopolysaccharidosis type VII (MPS VII). We used fetal neural stem cells derived from embryonic mouse striata and expanded *in vitro* by neurosphere formation as the source of graft materials. We transplanted neurospheres into the lateral ventricles of newborn MPS VII mice and found that donor cells migrated far beyond the site of injection within 24 h, and some of them could reach the olfactory bulb. A quantitative measurement indicated that the GUSB activity in the brain was 12.5 to 42.3% and 5.5 to 6.3% of normal activity at 24 h and 3 weeks after transplantation. In addition, histological analysis revealed a widespread decrease in lysosomal storage in the recipient's hippocampus, cortex, and ependyma. A functional assessment with novel-object recognition tests confirmed improvements in behavioral patterns. These results suggest that intracerebral transplantation of neural stem cells is feasible for treatment of CNS lesions associated with lysosomal storage disorders.

Key Words: neurosphere, mucopolysaccharidosis type VII, intracerebral transplantation

INTRODUCTION

Mucopolysaccharidosis type VII (MPS VII), or Sly syndrome, is a congenital lysosomal storage disorder (LSD) characterized by a systemic deficiency of β-glucuronidase (GUSB) activity [1]. This defect results in a progressive accumulation of undegraded glycosaminoglycans and subsequent lysosomal distension in multiple tissues, including the central nervous system (CNS). Enzyme replacement therapy and bone marrow transplantation are effective for correcting visceral manifestations of the disorder [2,3]. However, effective treatment of the CNS in patients with LSDs remains a major challenge.

With respect to cell therapy directed to the CNS in an MPS VII mouse, there are reports that the intracerebral transplantation of a genetically engineered neural progenitor [4] and retrovirally transduced syngeneic fibroblasts [5] corrected the lysosomal storage of the recipient's brain tissues. We also previously reported that adeno virally transduced rat amniotic epithelial cells injected into adult MPSVII mouse brains survived at the injection point for more than 9 weeks and the subsequent supply of enzyme resulted in pathological improvement in multiple areas of the MPS VII mouse brains [6].

In this study, we used fetal neural stem cells derived from embryonic mouse striata and expanded *in vitro* by neurosphere formation [7,8] as the source of graft materials. Neural stem cells are considered to be good candidates for cell therapy to treat CNS dysfunction. In fact, fetal neural tissues have been successfully used in human Parkinson disease patients [9,10]; however, as many as four to eight fetuses were required to obtain a sufficient number of cells to treat a single patient. Expansion of neural stem cells *in vitro* may overcome the above practical

Abbreviations used: CNS, central nervous system; GUSB, β-glucuronidase; MPS VII, mucopolysaccharidosis type VII.

1525-0016/$30.00

and ethical problems associated with fetal tissue transplantation and provide a source for graft material.

Here we describe improvements in the histopathology of the hippocampus, cortex, and ependyma and in nonspatial hippocampus-dependent learning and memory evaluated in a novel-object recognition test at 2 months after transplantation. These data suggest that early transplantation of neurospheres into the CNS may prevent or delay some of the progressive mental impairment associated with this LSD.

Results and Discussion

Production and Secretion Capacity of GUSB Enzymes by Neurospheres

The neurosphere is a floating cell cluster containing plenty of neural stem cells and is generated from a fetal mouse brain by neurosphere formation [7,8]. Briefly, when we culture fetal corpus striatum containing neural stem cells in a serum-free medium with growth factors, only neural stem cells can survive and form floating cell clusters called neurospheres. We initially determined the endogenous GUSB activity of neurospheres obtained from normal C57BL/6 mice. The GUSB activity of the neurosphere and its culture medium proved significantly higher than that of bone marrow cells (Figs. 1A and 1B). We also evaluated the difference in GUSB activity before and after differentiation. Most neurospheres differentiate into neural cells *in vivo* according to their microenvironments after transplantation [8]. The GUSB activities in differentiated cells and their culture media were almost equivalent to those of bone marrow cells, suggesting that the GUSB activity of the neurospheres was reduced, although it was maintained to the extent necessary for a therapeutic effect even after differentiation.

Intercellular Transport of the GUSB Enzyme

It is well known that most lysosomal enzymes can be taken up into cells by M6P receptor-mediated endocytosis, and that this process is efficiently blocked in the presence of M6P [11]. When we transferred the culture medium of neurospheres generated from C57BL/6 fetal mouse brains to dishes of the primary culture of neurons generated from C3H mice, 21.9% of the heat-stable C57BL/6 mouse-derived GUSB in the culture medium was internalized into the neurons in the absence of M6P (Fig. 1C). In contrast, it was significantly reduced in the presence of 10 mM M6P (Fig. 1C). This suggests that endocytosis by M6P receptors leads to the internalization of the GUSB enzyme secreted from the neurospheres to the neurons.

Lysosomal Enzyme Activities of the Neurosphere

Many LSDs display CNS symptoms. Most lysosomal enzymes have common transport systems mediated by the M6P receptor, and therefore the same transplantation strategy could be available if neurospheres can produce and secrete significant amounts of lysosomal enzymes. We determined the specific activities of several lysosomal enzymes in neurospheres and compared them with those in marrow stromal cells and human granulocytes. Similar or higher activities of lysosomal enzymes were identified in the neurosphere (Table 1).

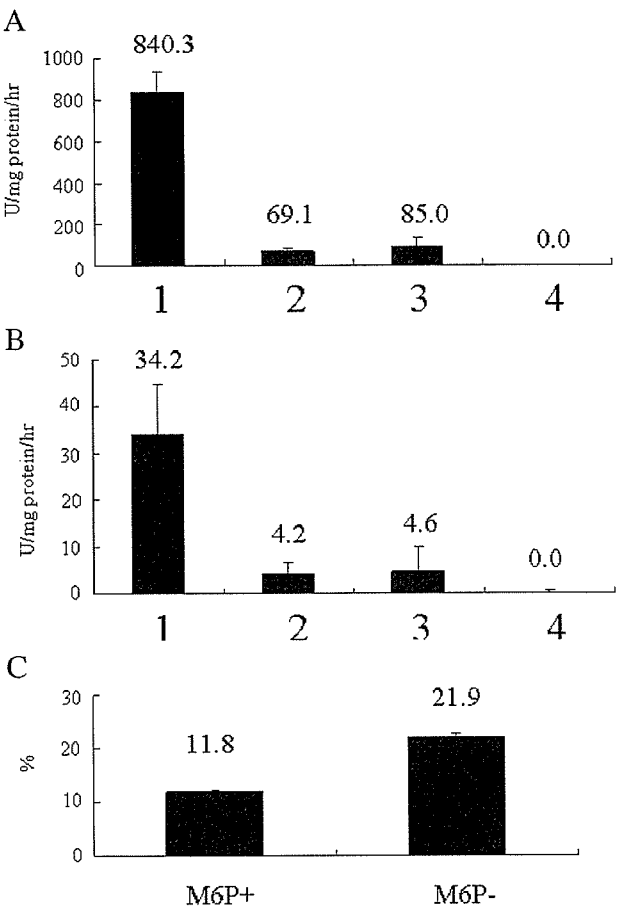

FIG. 1. Neurosphere GUSB activities and secretion via cell-to-cell transport. Lanes 1, neurospheres; 2, differentiated cells from neurospheres; 3, bone marrow cells; 4, 3521 cells (fibroblasts that originated from an MPS VII mouse). The GUSB activities of the neurosphere and its culture medium proved significantly higher than those of bone marrow cells. The GUSB activity in differentiated cells from neurospheres and that of its culture medium were almost equivalent to those of bone marrow cells. (A) GUSB activity in cell pellets of the neurosphere, bone marrow, and 3521 cells. (B) GUSB activity in a culture medium of the neurosphere, bone marrow, and 3521 cells at the time of the first passage. (C) Cell-to-cell transport of GUSB secreted from neurospheres. The ratio of the heat-stable GUSB activity in C3H mouse neural cells to the total heat-stable GUSB activity in the culture medium was calculated. The means ± standard errors are provided.

Distribution of Donor Cells after Neonatal Transplantation

We performed a syngeneic transplantation experiment using neurospheres obtained from CAG-EGFP transgenic

doi:10.1016/j.ymthe.2005.09.020

TABLE 1: Activities of lysosomal enzymes in the neurosphere and their related diseases[a]

Lysosomal enzyme	Disease	Neurosphere	MSC[b]	Granulocytes
α-L-Iduronidase	MPS I	39.2	57.4	56–201 (n = 6)
Iduronate sulfatase	MPS II	40.5	20	12–26 (n = 5)
Heparan-*N*-sulfatase	MPS IIIA	1.1	4.3	0.2–3 (n = 4)
GalNAc-6-*S*-sulfatase	MPS IVA	5.3	15.2	8.1–20 (n = 5)
Arylsulfatase B	MPS VI	55.3	15.5	9–32 (n = 5)
β-Glucosidase	Gaucher disease	3.0	6.5	0.2–0.6 (n = 100)
α-Galactosidase A	Fabry disease	189	68.8	49.8–116.4 (n = 48)
β-Galactosidase	MPS IVB	501	309	37.6–230.1 (n = 100)
α-Mannosidase	α-Mannosidosis	61.0	48.0	121.1–345.1 (n = 100)
β-Hexosaminidase	Sandhoff disease	1024	3062	401.7–1426.0 (n = 100)
β-Hexosaminidase A	Tay–Sachs disease	527	481	251.1–607.4 (n = 48)
Arylsulfatase A	MLD	435	278	109.0–217.2 (n = 100)

[a] We quantitatively assayed for a variety of lysosomal enzymes as well as GUSB. Several kinds of lysosomal enzymes were found to be high in the neurosphere. This result suggests that the neurosphere may be applied for the treatment of different types of congenital metabolic disorder. Data are given in nmol/mg protein/h. Enzyme activities in human granulocytes were measured as described elsewhere [27].
[b] MSC, marrow stromal cell.

mice (C57BL/6 background) as donor cells and newborn MPS VII mice as recipients. We injected 2.5–5 × 10^4 neurospheres (Fig. 2A) into the lateral ventricles of neonatal MPS VII mice within 1 to 3 days after delivery. A large number of donor cells were located mainly in the periventricular area at the hippocampus level in the brain, but a small number of GFP-positive cells were observed at varying distances away from the periventricular area at 24 h (Fig. 2B). We identified some of the GFP-positive cells in a linear formation at the level of the olfactory bulb, indicating a specific manner of migration in this area that is referred to as chain migration [12] (Fig. 2C). The overall distribution of the donor cells throughout the brain was essentially identical in all mice examined histologically (n = 3), with findings similar to previous reports [4,13–15]. There was evidence of GUSB

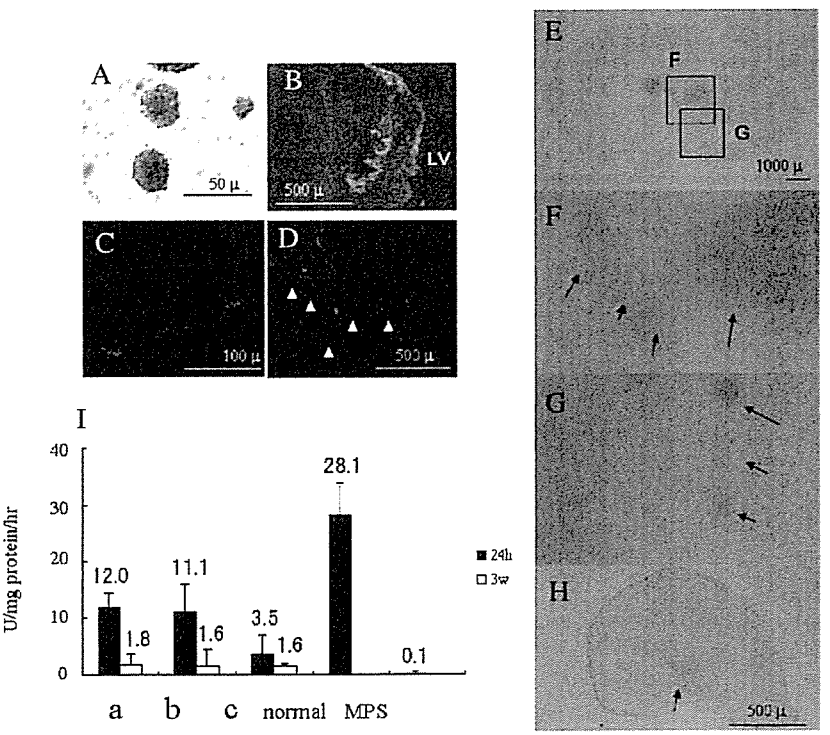

FIG. 2. Distribution of the donor cells in a mouse brain following transplantation of neurospheres. (A) Neurospheres generated from GFP transgenic mice under a fluorescence microscope. (B) A slice at the hippocampus level in the brain at 24 h after transplantation under a fluorescence microscope. GFP-positive cells were located mainly in the periventricular area. (C) A slice at the olfactory bulb level in the brain at 24 h after transplantation. GFP-positive cells were also detected under a fluorescence microscope; some of them were found to form a line (a chain migration). (D) A slice at the hippocampus level in the brain under a fluorescence microscope at 3 weeks after transplantation. GFP-positive cells were found to be branched and to form a network with the recipient brain tissue. (E–H) The brain of an MPS VII mouse at 24 h after transplantation of neurospheres. The recipient brain was stained red by GUSB staining in accordance with the GFP-positive area. (E–G) Coronal sections of the telencephalon at the caudal level. (H) Olfactory bulb. (I) Quantitative determination of the GUSB activity was performed at 24 h and 3 weeks after transplantation. The brains of the transplant recipients were divided coronally into three parts and quantitatively assayed for GUSB activity (n = 3). The regions used for evaluation at the designated times were defined by anatomical landmarks in the anterior-to-posterior plane: a, olfactory bulbs; b, caudal edge of the olfactory bulbs to the rostral edge of the hippocampus; c, hippocampus to the posterior colliculus. The cerebellum was dissected free and was not included in the assay.

staining in accordance with the GFP-positive area, indicating a rise in GUSB activity (Figs. 2E–2H).

We previously reported that neurosphere-derived donor neurons extend their processes into the host tissues and form a synaptic structure [8]. The GFP-positive cells had extended their processes and formed synaptic structures as well 3 weeks after transplantation (Fig. 2D). These data suggest that the donor cells migrated from the periventricular area and some of them reached the olfactory bulb as early as 24 h after transplantation.

Quantitative Gusb Assay in Transplanted Mouse Brains

We divided the brains of the transplant recipients coronally into three parts and quantitatively assayed them for GUSB activity at 24 h (n = 3) and 3 weeks (n = 3) after transplantation (Fig. 2I). GUSB activity was 12.5 to 42.3% of normal activity at 24 h. There was 5.5 to 6.3% of normal activity at 3 weeks after transplantation. This is an amount at which that lysosomal distensions in the neuron and glia could also be reversed [16]. These results imply that donor cells provided the recipient brain with GUSB activity to the extent that lysosomal storage in the recipient brain could be prevented for at least 3 weeks.

Histological Analysis and Tumorigenesis Assessment of the Treated Mice

We tested the treated MPS VII mice for reduction of lysosomal distensions in the neurons and glia at 2 months after transplantation (n = 2) (Figs. 3 and 4). We performed a histological analysis on hippocampus, cortex, and ependyma using an optical microscope (hippocampus, cortex, and ependyma) and an electron microscope (cortex). In the hippocampus of the untreated MPS VII mice, most of neurons contained marked cytoplasmic vacuolation (lysosomal storage) as well as astrocytes. In contrast, those of the treated hippocampuses were almost eliminated especially from neurons in this area. In the cortices, we also observed extensive neuronal and glial vacuolation, and the treatment reduced them remarkably as well. An electron microscope demonstrated that lysosomal storage in some neurons was completely eliminated in this area

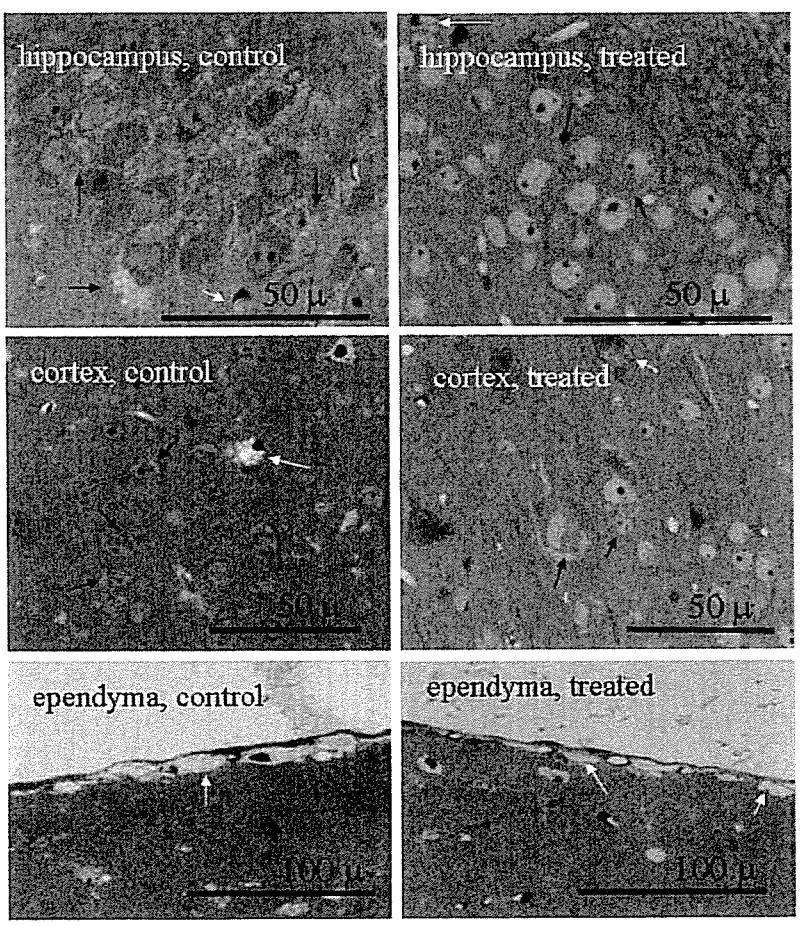

FIG. 3. Toluidine blue-stained, 0.5-μm-thick sections from the hippocampus, cortex, and ependyma are from 2-month-old MPS VII mice (n = 2). Intraventricular injection of neurospheres decreases lysosomal storage in the hippocampus, cortex, and ependyma. Black arrows indicate distended vacuoles in neurons; white arrows indicate storage in glia.

doi:10.1016/j.ymthe.2005.09.020

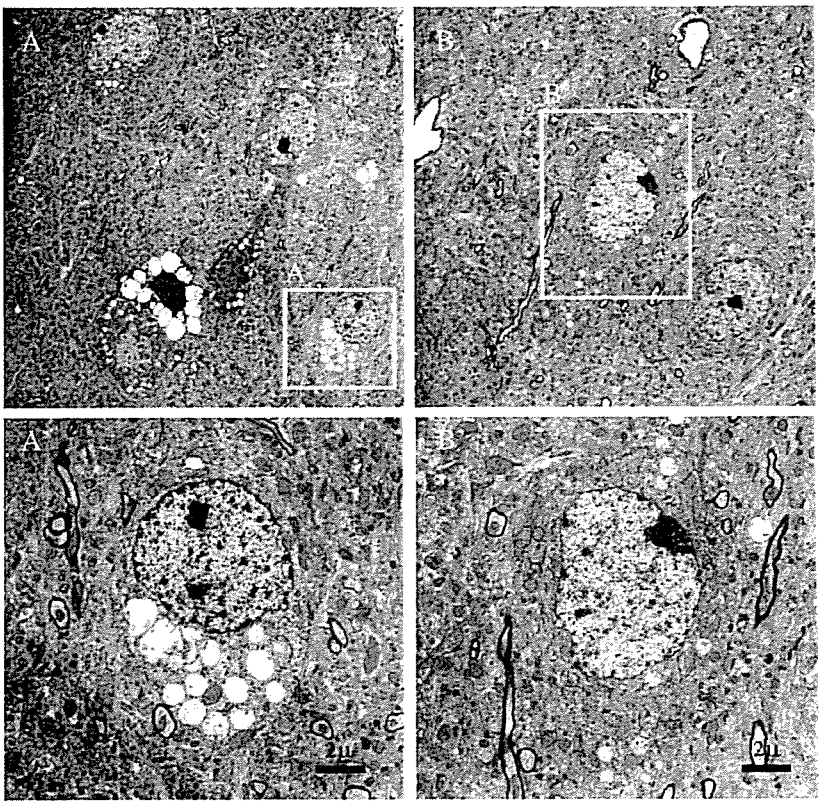

FIG. 4. Electron microscopic analysis of lysosomal storage in a mouse brain following transplantation of neurospheres. (A) Cortex of a control untreated MPS VII mouse at 2 months after transplantation. Abundant white cytoplasmic vacuoles represent distended lysosomes. (B) Cortex of a MPS VII mouse at 2 months after transplantation. Lysosomal storage granules in this area were remarkably reduced in size and number, and those in some neurons were completely eliminated. (A′ and B′) Magnified photographs of the circumscribed areas in (A) and (B).

(Fig. 4). In the ependyma, the amount of storage appeared to be significantly reduced in the treated mice. To evaluate quantitatively the improvement of the pathology in the treated mice, we counted neurons and glia containing apparent vacuolation in each hippocampus and cortex of the treated and the untreated mice ($n = 2$, total 300 cells in each area) in the HPF (×600). In both areas, we observed a remarkable decrease in the number of neurons and glia with apparent lysosomal storage, and this finding was almost equal in two treated mice, indicating an improvement of the pathology in the treated mouse brains (Table 2). We carefully assessed all transplanted mice for the presence of tumorigenesis. We dissected the brains of the dead mice during the course of the study and macroscopically analyzed them for tumor formation, but we could not identify any tumor formation among them.

TABLE 2: The percentage of cells with apparent vacuolization in the brain of MPS VII mice treated with intraventricular injection of neurospheres[a] ($n = 2$)

	Untreated	Treated
Hippocampus	89.3%	17.3%
Neuron	90%	18.4%
Glia	92%	13.9%
Cortex	42%	15.3%
Neuron	37.7%	11.7%
Glia	55.6%	30%

[a] Toluidine blue sections of hippocampus and cortex were analyzed for lysosomal distention, and we counted neurons and glia containing much vacuolation in 300 cells in each of hippocampus and cortex in the HPF (×600).

Mouse Hearing Acuity Assessment

Measurements of the auditory brain-stem response (ABR) have been useful in assessing functional improvements after treatment [17]. We tested three treated MPS VII mice, three untreated MPS VII mice, and three C57BL/6 mice. There was no significant difference in the ABR thresholds among the treated and the untreated MPS VII mice (Fig. 5A). It is well known that malalignment and focal loss of stereocilia occur as the disease progresses, leading to a sensorineural hearing loss [18]. As the ABR was performed at 2 months, it may have been too early to assess the sensorineural hearing loss.

Behavioral Assessment

We used a novel-object recognition test, a tool for studying nonspatial hippocampus-dependent memory, to determine whether an improvement in mental status could be achieved by transplantation [19–21]. We carried out this test as described [19] with several modifications at 2 months after transplantation ($n = 3$). We used normal siblings of the treated MPS VII mice as the control mice. In summary, after the mice were habituated to an open field, two yellow objects (A, B) were placed diagonally in

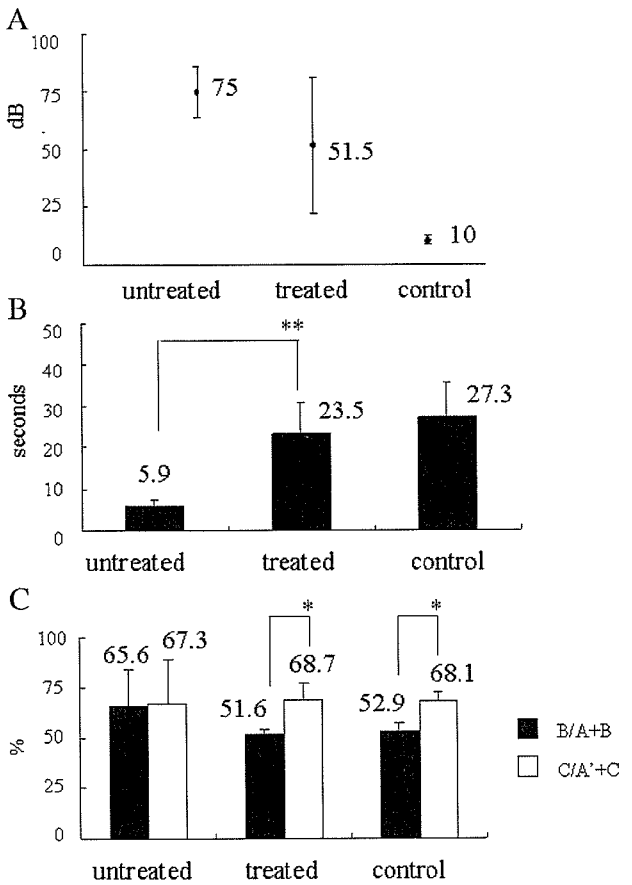

FIG. 5. Assessment of the functional recovery at 2 months after transplantation. (A) Auditory-evoked brain-stem responses. The decibels required to elicit ABR at the broadband (clicks) were evaluated among three normal mice, three treated MPS VII mice, and three untreated MPS VII mice at 2 months after transplantation. There was no significant difference in the ABR thresholds among the treated MPS VII mice and the untreated MPS VII mice. (B) The novel-object recognition test. The mice were assessed for an improvement in hippocampus-dependent nonspatial memory by a novel-object recognition test ($n = 3$). The total time spent exploring objects on day 4 (=A + B) in the treated mice was significantly longer than that for the untreated mice. (**$P < 0.01$). (C) The novel-object recognition test (retention test). The percentage of time spent in exploring B as a portion of the total object exploration time on day 4 [B/(A + B)] was compared with that of C (the novel object) on day 5 [C/(A′ + C)]. C/(A′ + C) in the C57BL/6 and the treated mice was significantly greater than B/(A + B). This suggests that the normal mice and the treated mice spent a significantly longer time exploring the novel object, revealing that both groups had a significant preference for exploring the novel object. The means ± standard errors are provided.

the open field on day 4, and the mice were allowed to explore them for 10 min. Object B was replaced with a novel object (C) and the other object was replaced with a replica (A′) on day 5, and the mice were again allowed to explore them for 10 min. Normal animals prefer to explore the novel object more than the familiar object. From the degree of preference for exploration of the new object, it can be inferred that they retained a memory of the familiar object. The total time spent exploring object A or B on day 4 (=A + B) was 27.3 ± 8.4 s in the normal mice, 23.5 ± 7.4 s in the treated mice, and 5.9 ± 1.6 s in the untreated mice (Fig. 5B), indicating that the normal and the treated mice had the same levels of motivation, curiosity, and interest in exploring objects. Next, to evaluate preferential exploration of the novel object, we compared the percentage of time spent exploring object B as a portion of the total object-exploration time on day 4 [=B/(A + B)] with that of object C (the novel object) on day 5 [=C/(A′ + C)] (Fig. 5C). C/(A′ + C) in the normal and the treated mice was significantly greater than B/(A + B) [normal mice, B/(A + B) = 52.9 ± 3.9%, C/(A′ + C) = 68.1 ± 4.4%; treated mice, B/(A + B) = 51.6 ± 2.8%, C/(A′ + C) = 68.7 ± 8.4% of the exploration time]. This indicates that the normal mice and the treated mice spent a significantly longer time exploring the novel object, revealing that both groups exhibited a significant preference for exploring it. These results indicate that the treated mice have the same level of nonspatial hippocampus-dependent memory as the normal mice. But we cannot completely deny the possibility that the vision had an influence on this improvement of a novel object test.

To date, there are reports demonstrating an improvement in behavior of treated MPS VII mice assessed by a Morris water maze test [22,23]. We used a novel-object test because it is very easy and less of a burden on the mice than the Water maze test. Consequently, it is easily applicable to mice with motility disturbance, and we thought we could maximize mouse performance associated with visual recognition memory. The long-term effects of this treatment have not been examined in detail. The treated mice lived to 7 months of age at most. Transplantation of neurospheres did not extend the life span of MPS VII mice. Life span may be dependent on systemic lysosomal storage other than the CNS.

In summary, our results demonstrated that after transplantation of *in vitro*-expanded neurospheres into the neonatal ventricle of MPS VII mice brains, the transplant donor cells migrated along established routes and integrated into the recipient's brain. The treated mice exhibited improved cognitive functions as measured by a novel-object recognition test, which was consistent with histological evidence of reduced lysosomal storage in the brain tissue.

MATERIALS AND METHODS

Animals. Syngeneic MPS VII (*mps/mps*) mice were obtained from a pedigree colony of B6.C-H-2^{bml}/ByBir-gus^{mps}/+ mice maintained at our facility [6]. Normal C3H mice were purchased from Shizuoka Laboratory Animal Center (Shizuoka, Japan). CAG-EGFP transgenic mice were originally generated by Endo *et al.* [24,25]. All mice were maintained and treated in accordance with the guidelines of the animal committee of the facility.

Isolation, primary cultures, and passaging procedures of neurospheres. Embryos were removed from CAG-EGFP transgenic mice on day 14.5 of pregnancy. The corpus striatum was dissected and prepared as described

doi:10.1016/j.ymthe.2005.09.020

elsewhere [7]. Neurospheres were cultured in the medium described below at 37°C with 5% CO_2 at a concentration of 2×10^5 cells/ml in the primary culture. The culture medium was DMEM/F12 supplemented with the hormone mixture used by Reynolds and Weiss [7]. Passages were performed once per week. Neurospheres were used for the transplantation after the second to fifth passage.

Cell-to-cell transport of GUSB secreted from neurospheres. We evaluated *in vitro* the uptake ratio of the GUSB enzyme secreted from neurospheres of C57BL/6 mice into neural cells of C3H mice by using the difference in the heat stability of GUSB proteins between C57BL/6 mice and C3H mice. In brief, GUSB activity of C57BL/6 mice was reduced by only 30% after a 2-h incubation at 65°C [11]. In contrast, GUSB activity of C3H mice was decreased markedly after this procedure. We prepared a culture medium of neurospheres from C57BL/6 mice after 1 week incubation. We replaced the medium of primary neurons of C3H mice with the above medium, continued to culture in the presence or absence of M6P, and harvested 12 h later. Heat-stable GUSB activity in the homogenates of C3H mouse neurons was measured after a 2-h incubation at 65°C.

Quantitative analysis of GUSB activity. GUSB activity in tissues and cell homogenates was quantified using a fluorometric assay described previously [26]. Neurospheres were quantitatively analyzed after the second to fifth passage. Differentiated cells were obtained from neurospheres by converting the culture medium into DMEM +10% FBS. We had previously demonstrated that these cells differentiated into neurons, astrocytes, and oligodendrocytes by immunological staining (data not shown). Bone marrow was isolated from C57BL/6 mice and cultured in DMEM +10% FBS. Attached cells were collected after the second to fifth passage and analyzed for GUSB activity.

Histochemical detection of GUSB activity. The mice were perfused with physiological saline and subsequently with 4% paraformaldehyde before preparation of the brains. The brains were equilibrated in a 30% sucrose solution (4°C, overnight), frozen in M-1 embedding matrix (Shandon, Pittsburgh, PA, USA), and then sectioned on a cryostat. Histochemical analysis of GUSB activity was performed on 20-μm-thick frozen sections using naphthol AS-BI β-D-glucuronide (Sigma) as a substrate [26].

Lysosomal enzyme activities of the neurosphere. Lysosomal enzyme activities in neurospheres, the marrow stromal cells, and human granulocytes were quantified using a fluorometric assay as described with some modification [27].

Histopathological analysis of lysosomal storage. Histopathology in neurons and glia was analyzed at 2 months after transplantation, corresponding to 2 months of age ($n = 2$). Tissues were isolated from the mice and immediately immersed in cold 2% glutaraldehyde in 0.1 M cacodylate buffer, postfixed in 1% osmium tetroxide, dehydrated through a graded series of ethanol solutions, and embedded in Spurr's Medium (Polyscience, Warrington, PA, USA). Toluidine blue-stained, 0.5-μm-thick sections were analyzed for evidence of lysosomal storage in hippocampus, cortex, and ependyma. Cytoplasmic lysosomal distensions in the cortex were also evaluated with an electron microscope.

Auditory brain-stem responses. ABR examination was performed 20 min after anesthesia in a quiet room, as described previously [28].

Novel-object recognition tests. Novel-object recognition tests evaluate nonspatial hippocampus-dependent learning and memory [19–21] and were performed as described [19] with several modifications. The mice were habituated in an open field over a 2-day preexposure (day 1 for 5 min and day 3 for 5 min). Two yellow objects (A and B) were placed diagonally in the open field (15 cm away from the walls) on day 4, and the mice were allowed to explore them for 10 min. Object B was replaced with the novel object (C), and the other object was replaced with a replica (A′) on day 5, and the mice were again allowed to explore them for 10 min. Recognition of the familiar object was scored by preferential exploration of the novel object. A + B represents total time exploring on day 4. A′ + C represents total time exploring on day 5. B/(A + B) represents the ratio of time exploring object B to total time exploring on day 4. C/(A′ + C) represents the ratio of time exploring object C to total time exploring on day 5.

ACKNOWLEDGMENTS

This work was supported by a grant from Terumo Foundation Life Science Foundation to HO, and a grant from the 21st Century COE program of the Japanese Ministry of Education, Culture, Sports, Science and Technology Ministry to Keio University.

RECEIVED FOR PUBLICATION APRIL 27, 2005; REVISED SEPTEMBER 13, 2005; ACCEPTED SEPTEMBER 27, 2005.

REFERENCES

1. Sly, W. S., Quinton, B. A., McAllister, W. H., and Rimoin, D. L. (1973). β-Glucuronidase deficiency: report of clinical, radiologic, and biochemical features of a new mucopolysaccharidosis. *J. Pediatr.* **82:** 249–257.
2. Vogler, C., *et al.* (1993). Enzyme replacement with recombinant beta-glucuronidase in the newborn mucopolysaccharidosis type VII mouse. *Pediatr. Res.* **34:** 837–840.
3. Birkenmeier, E. H., *et al.* (1991). Increased life span and correction of metabolic defects in murine mucopolysaccharidosis type VII after syngeneic bone marrow transplantation. *Blood* **78:** 3081–3092.
4. Snyder, E. Y., Taylor, R. M., and Wolfe, J. H. (1995). Neural progenitor cell engraftment corrects lysosomal storage throughout the MPS VII mouse brain. *Nature* **374:** 367–370.
5. Taylor, R. M., and Wolfe, J. H. (1997). Decreased lysosomal storage in the adult MPS VII mouse brain in the vicinity of grafts of retroviral vector-corrected fibroblasts secreting high levels of β-glucuronidase. *Nat. Med.* **3:** 771–775.
6. Kosuga, M., *et al.* (2001). Engraftment of genetically engineered amniotic epithelial cells corrects lysosomal storage in multiple areas of the brain in mucopolysaccharidosis type VII mice. *Mol. Ther.* **3:** 139–148.
7. Reynolds, B. A., and Weiss, S. (1992). Generation of neurons and astrocytes from isolated cells of adult mammalian central nervous system. *Science* **255:** 1707–1710.
8. Ogawa, Y., *et al.* (2002). Transplantation of in vitro-expanded fetal neural progenitor cells results in neurogenesis and functional recovery after spinal cord contusion injury in adult rats. *J. Neurosci. Res.* **69:** 925–933.
9. Lindvall, O., *et al.* (1990). Grafts of fetal dopamine neurons survive and improve motor function in Parkinson's disease. *Science* **247:** 574–577.
10. Freed, C. R., *et al.* (1992). Survival of implanted fetal dopamine cells and neurologic improvement 12 to 46 months after transplantation for Parkinson's disease. *N. Engl. J. Med.* **327:** 1549–1555.
11. Gwynn, B., Lueders, K., Sands, M., and Birkenmeier, E. H. (1998). Intracisternal A-particle element transposition into the murine β-glucuronidase gene correlates with loss of enzyme activity: a new model for β-glucuronidase deficiency in the C3H mouse. *Mol. Cell. Biol.* **18:** 6474–6481.
12. Lois, C., and Alvarez-Buylla, A. (1994). Long-distance neuronal migration in the adult mammalian brain. *Science* **264:** 1145–1148.
13. Ourednik, V., *et al.* (2001). Segregation of human neural stem cells in the developing primate forebrain. *Science* **293:** 1820–1824.
14. Meng, X. L., Shen, J. S., Ohashi, T., Maeda, H., Kim, S. U., and Eto, Y. (2003). Brain transplantation of genetically engineered human neural stem cells globally corrects brain lesions in the mucopolysaccharidosis type VII mouse. *J. Neurosci. Res.* **74:** 266–277.
15. Tamaki, S., *et al.* (2002). Engraftment of sorted/expanded human central nervous system stem cells from fetal brain. *J. Neurosci. Res.* **69:** 976–986.
16. Sferra, T. J., Backstrom, K., Wang, C., Rennard, R., Miller, M., and Hu, Y. (2004). Widespread correction of lysosomal storage following intrahepatic injection of a recombinant adeno-associated virus in the adult MPS VII mouse. *Mol. Ther.* **10:** 478–491.
17. Kopen, G. C., Prockop, D. J., and Phinney, D. G. (1999). Marrow stromal cells migrate throughout forebrain and cerebellum, and they differentiate into astrocytes after injection into neonatal mouse brains. *Proc. Natl. Acad. Sci. USA* **96:** 10711–10716.
18. Sands, M. S., Erway, L. C., Vogler, C., Sly, W. S., and Birkenmeier, E. H. (1995). Syngeneic bone marrow transplantation reduces the hearing loss associated with murine mucopolysaccharidosis type VII. *Blood* **86:** 2033–2040.
19. Dulawa, S. C., Grandy, D. K., Low, M. J., Paulus, M. P., and Geyer, M. A. (1999). Dopamine D4 receptor-knock-out mice exhibit reduced exploration of novel stimuli. *J. Neurosci.* **19:** 9550–9556.
20. Soderling, S. H., *et al.* (2003). Loss of Wave-1 causes sensorimotor retardation and reduced learning and memory in mice. *Proc. Natl. Acad. Sci. USA* **100:** 1723–1728.
21. Rompon, C., *et al.* (2000). Enrichment induces structural changes and recovery from nonspatial memory deficits in CA1 NMDAR-knockout mice. *Nat. Neurosci.* **3:** 238–244.
22. O'Connor, L. H., *et al.* (1998). Enzyme replacement therapy for murine mucopolysaccharidosis type VII leads to improvements in behavior and auditory function. *J. Clin. Invest.* **101:** 1394–1400.

23. Brooks, A. I., *et al.* (2002). Functional correction of established central nervous system deficits in an animal model of lysosomal storage disease with feline immunodeficiency virus-based vectors. *Proc. Natl. Acad. Sci. USA* **99:** 6216–6221.
24. Hayakawa, M., *et al.* (2002). Muscle-specific exonic splicing silencer for exon exclusion in human ATP synthase gamma-subunit pre-mRNA. *J. Biol. Chem.* **277:** 6974–6984.
25. Ichida, M., *et al.* (2000). Differential regulation of exonic regulatory elements for muscle-specific alternative splicing during myogenesis and cardiogenesis. *J. Biol. Chem.* **275:** 15992–16001.
26. Wolfe, J. H., and Sands, M. S. (1996). Murine mucopolysaccharidosis type VII: a model system for somatic gene therapy of the central nervous system. In *Gene Transfer into Neurons: Towards Gene Therapy of Neurological Disorders* (P. Lowenstein and L. Enquist, Eds.), Wiley, Essex.
27. Den Tandt, W. R., and Scharpe, S. (1991). Characteristics of hexosaminidase A in homogenates of white blood cells using methylumbelliferyl-*N*-acetyl-β-D-glucosaminide-6-sulphate as substrate. *Clin. Chim. Acta* **199:** 231–236.
28. Willott, J. F., Turner, J. G., Carlson, S., Ding, D., Bross, L. S., and Falls, W. A. (1998). The BALB/c mouse as an animal model for progressive sensorineural hearing loss. *Hear. Res.* **115:** 162–174.

JOURNAL OF CELLULAR PHYSIOLOGY 208:188–194 (2006)

Increased Mobilization of c-kit$^+$ Sca-1$^+$ Lin$^-$ (KSL) Cells and Colony-Forming Units in Spleen (CFU-S) Following De Novo Formation of a Stem Cell Niche Depends on Dynamic, But Not Stable, Membranous Ossification

KAZUNARI NAGAYOSHI,[1,2] HIROYUKI OHKAWA,[2] KEIGO YOROZU,[2] MASATO HIGUCHI,[2] SAYUMI HIGASHI,[2] NAOKI KUBOTA,[2] HIROYASU FUKUI,[2] NOBUO IMAI,[2] SATOSHI GOJO,[3] JUN-ICHI HATA,[1] YOSHIRO KOBAYASHI,[4] AND AKIHIRO UMEZAWA[1]*

[1]*Department of Reproductive Biology and Pathology, National Research Institute for Child Health and Development, Tokyo, Japan*

[2]*Chugai Pharmaceutical Co., LTD, Fuji Gotemba Research Institute, Gotemba, Shizuoka, Japan*

[3]*Department of Cardiovascular Surgery, Saitama Medical Center, Kawagoe, Japan*

[4]*Department of Biomolecular Science, Faculty of Science, Toho University, Chiba, Japan*

Stem cells are thought to inhabit in a unique microenvironment, known as "niche," in which they undergo asymmetric cell divisions that results in reproducing both stem cells and progenies to maintain various tissues throughout life. The cells of osteoblastic lineage have been identified as a key participant in regulating the number of hematopoietic stem cells (HSCs). HSCs receive their regulatory messages from the microenvironment in the bone marrow. This would account for a reason why the localization of hematopoiesis is usually restricted in the bone marrow. To clarify the above possibility we employed a cell implantation-based strategy with a unique osteoblast cell line (KUSA-A1) derived from a C3H/He mouse. The implantation of KUSA-A 1 cells resulted in the generation of ectopic bones in the subcutaneous tissues of the athymic BALB/c nu/nu mice. Subsequently the mice obtained a greater amount of the bone marrow than normal mice, and they showed an increased number of HSCs. These results indicate that the newly generated osteoblasts-derived ectopic bones are responsible for the increase in the number of the HSC population. Furthermore, the increased number of HSCs directly correlates with both the magnitude of dynamic osteogenic process and the size of the newly generated bone or "niche." J. Cell. Physiol. 208: 188–194, 2006. © 2006 Wiley-Liss, Inc.

Stem cell with potential for self-renewal and multilineage differentiation can be identified in various self-renewing tissues, including epidermis, intestinal epithelium, and testis, and hematopoietic stem cells (HSCs) are also capable of both self-renewal and multipotency (Ikehara, 2000; Weissman, 2000). The most important experimental evidence for the existence of such cells is the ability of a single bone-marrow-derived cell to reconstitute long-term hematopoiesis in lethally irradiated recipients (Till and McCulloch, 1961; Siminovitch et al., 1963; Till et al., 1964; Matsuzaki et al., 2004). Molecular markers that characterize transplantable cells with stem cell potential and allow their selective purification have been identified, and this achievement has been important to progress both applied and basic science (Spangrude et al., 1988; Goodell et al., 1996). As an example, CD34$^-$, c-kit$^+$, Sca-1$^+$, and Lin$^-$ cells have been identified as the most primitive HSCs (Osawa et al., 1996).

Stem-cell fate decisions in the developing embryo are governed by complex interplays between cell-autonomous signals and stimuli from the surrounding tissues. Stem cells are thought to inhabit in a unique microenvironment, known as "niche," in which they undergo asymmetric divisions that generate both stem cells and progenies to maintain the tissue throughout life (Dzierzak et al., 1998; Matsuzaki et al., 2004). HSCs migrate from the yolk sac to the liver during early development, and they ultimately settle in the bone marrow and spleen of the adult. The bone marrow and spleen serve as the microenvironment that supports the HSCs via cytokines, membrane-bound molecules, and gap junctions. And the classical experiment on HSC-colony formation by Till and McCulloch (1961) showed that reconstitution of hematopoiesis takes place only in hematopoietic organs. The niche hypothesis was first proposed by Schöfield, 1978, and it is supported by the evidence that HSCs have been successfully maintained in co-culture systems with marrow-derived stromal cells in vitro. Steel mice (Sl/Sld) have a mutation at the Sl locus, and spleen colonies cannot be produced in the mice when transplanted with normal marrow cells.

This article includes Supplementary Material available from the authors upon request or via the Internet at http://www.interscience.wiley.com/jpages/0021-9541/suppmat.

Contract grant sponsor: Ministry of Education, Culture, Sports, Science, and Technology (MEXT) of Japan; Contract grant numbers: 14081208, 13470053, 14657051); Contract grant sponsor: Health and Labour Sciences Research Grants; Contract grant numbers: H-14-trans-003, KH71064; Contract grant sponsor: Pharmaceuticals and Medical Devices Agency; Contract grant number: 02-2.

*Correspondence to: Akihiro Umezawa, Department of Reproductive Biology and Pathology, National Research Institute for Child Health and Development, 2-10-1 Okura, Setagaya-ku, Tokyo 157-8535, Japan. E-mail: umezawa@1985.jukuin.keio.ac.jp

Received 26 July 2005; Accepted 13 February 2006

DOI: 10.1002/jcp.20652

Steel mice have a defect in the hematopoietic microenvironment, or the niche, where marrow stromal cells constitute (Harrison and Russell, 1972).

Bone marrow stromal cells are capable of differentiating into adipocytes, endothelial cells, chondrocytes, and osteoblasts (Pittenger et al., 1999). They are also capable of transdifferentiating into cardiomyocytes, skeletal myocytes, and neurons when exposed to inducers in vitro and in vivo (Umezawa et al., 1992; Makino et al., 1999; Kohyama et al., 2001; Takeda et al., 2004; Mori et al., 2005; Terai et al., 2005). Previous studies on the role of stromal cells in supporting HSCs have mainly been based on in vitro culture. The trabecular area of cancellous bone is the primary site of HSCs. They arise next to the inner surface of bone, and then migrate towards the blood vessels at the center of the bone marrow cavity as they mature. Since the 1970s, efforts to characterize the HSC niche have been focusing on developing systems in vitro that mimic some of the features of stem cell–niche interactions in vivo, and single clones of stromal cells have been found to be capable of supporting HSC self-renewal and differentiation in vivo (Okada et al., 1991, 1992). Osteoblastic marrow stromal cells are a regulatory component of the HSC niche in vivo that influences stem cell function, and some stromal cell clones are part of the bone-forming 'osteoblastic' lineage, which is consistent with a notion that osteoblasts may be a component of the HSC niche in vivo (Lord, 1990; Yoshimoto et al., 2003).

In the present study, we demonstrate that KUSA-A1 osteoblasts, whose number has been increased by local injection into the tissues, support an increase in the number of HSCs in both bone marrow and peripheral blood as a result of an increase in size of the microenvironment or niche in vivo. We provide in vivo evidence that shows an extra osteogenic process independent from that in the normal bone affects the reproduction of stem cells.

MATERIALS AND METHODS

Mice and their major histocompatibility complex (MHC) Class I

BALB/c nu/nu (H-2d), BALB/c (H-2d), C57BL/6N (H-2b), and C3H/He (H-2k) mice were obtained from Clea Japan Inc (Tokyo, Japan).

Cell lines and cell culture

KUSA-A1 cells, that was derived from a C3H/He mouse, were maintained in the M061101 medium (okada@med-shirotori.co.jp, MED SHIROTORI Co., Ltd., Tokyo) on 100 mm culture dishes (Falcon 3003; Becton Dickinson Labware, Bedford, MA) at 37°C under a humidified atmosphere of 5% CO_2. ST-2 cells were obtained from the RIKEN cell bank, Japan, and were maintained in RPMI 1640 (Invitrogen Corporation, Auckland, New Zealand) supplemented with 10% FCS and 10^{-5}M of 2-ME (GIBCO BRL) at 37°C under a humidified atmosphere of 5% CO_2 in air.

Cell transplantation

Freshly scraped confluent cells (5×10^6) were subcutaneously implanted into BALB/c nu/nu mice (Clea). These animals were sacrificed by cervical dislocation between 3 and 10 weeks after implantation.

Antibodies

Phycoerythrin (PE)-conjugated antibodies to CD4, CD8, CD3, B220, Mac-1, Gr-1, and Tre119 (Pharmingen, San Diego, CA), fluorescein isothiocyanate (FITC)-conjugated antibody to CD34, H-2k (Pharmingen), allophycocy antim (APC)-conjugated antibody to c-kit (Pharmingen), Sca-1 biotinate antibody (Pharmingen), and antibody to CD16/32 (Fc III/II receptor; 1: 100; Fcblock; Pharmingen) were used for flow cytometric analysis.

Flow cytometric analysis

The monoclonal antibodies (mAbs) were either biotinylated or fluoresceinated. Biotinylated mAbs were detected with streptavidin-conjugated Red 613 (Invitrogen Corporation). Cells were incubated for 30 min on ice with CD16/32 (Fc III/II receptor; 1: 100; Fcblock) before staining with the first antibody. Cells were stained with the first antibody, incubated for 30 min on ice, and then washed twice with washing buffer. The secondary antibody was added, and after incubating the cells for 30 min on ice, they were washed twice with washing buffer and suspended in washing buffer. KUSA-A1 cell suspensions were prepared from monolayer cultures by exposure to trypsin (0.02% for 3 min at 37°C), followed by two washes in cold PBS plus 2% FCS and 0.01% sodium azide. After staining with a series of monoclonal antibodies according to manufacturer's protocol, cells were analyzed by fluorescence-activated cell sorter (FACS) with the FACS vantage system (Becton Dickinson, San Jose, CA).

Colony-forming unit in spleen (CFU-S) assay of hematopoietic cells obtained from ectopic bone

Freshly scraped confluent KUSA-A1 cells (5×10^6) were subcutaneously implanted into BALB/c nu/nu mice (Clea). Hematopoietic cells were obtained from ectopic bone marrow generated by KUSA-A1 cells, and were assayed for CFU-S. Bone marrow cells (5×10^5) were implanted into lethally irradiated BALB/c mice, and the number of colonies (Day 12 CFU-S) was counted 12 days after transplantation. Day 12 CFU-S including erythrocytic, granulocytic, megakaryocytic, and lymphocytic lineages are derived from multipotent HSCs and are more potent in terms of repopulating ability than day 8 CFU-S.

Soft X ray system

BALB nu/nu mice were examined by whole body soft X-ray radiography at 25.0 kV and 3.0 mA for 10 sec (SRO-iM50, Sofron, Tokyo) with X-ray RX film (Fuji Photofilm GmbH, Düsseldorf, Germany).

RESULTS

Induction of hematopoiesis by KUSA-A1 cells

When KUSA-A1 cells were implanted into the subcutaneous tissue, solid hard masses (Fig. 1A) were detected 5 weeks later as electron-dense nodules by soft X-ray analysis (Fig. 1B) at all implantation sites, that is, in the dermal tissue right beneath the cutaneous muscle. Histological examination revealed that the implanted cells survived, and some of them showed mitotic figures (Fig. 1C(a)). At 2 weeks following implantation, an osteogenic matrix was formed in the interstitium, but its matrix formation was still scanty (Fig. 1C(b)). And marked formation of capillary vessels containing erythrocytes in their lumen was observed. At 3 weeks, dense immature bone trabeculae with prominent vascular formation and osteoclast induction were seen (Fig. 1C(c)). By 4 weeks, mature bone trabeculae and sinusoids formed (Fig. 1C(d)), and there were mature granulocytic cells in the marrow space. Hematopoiesis began by 3–5 weeks after implantation.

To determine whether the size of the bone generated by KUSA-A1 cells depends on the implanted cell number, we implanted different numbers of KUSA-A1 cells into subcutaneous tissue (Fig. 1D). The results showed that bone size was clearly depending on the number of cells implanted. Nevertheless, hematopoiesis occurred regardless of the number of cells implanted and bone size.

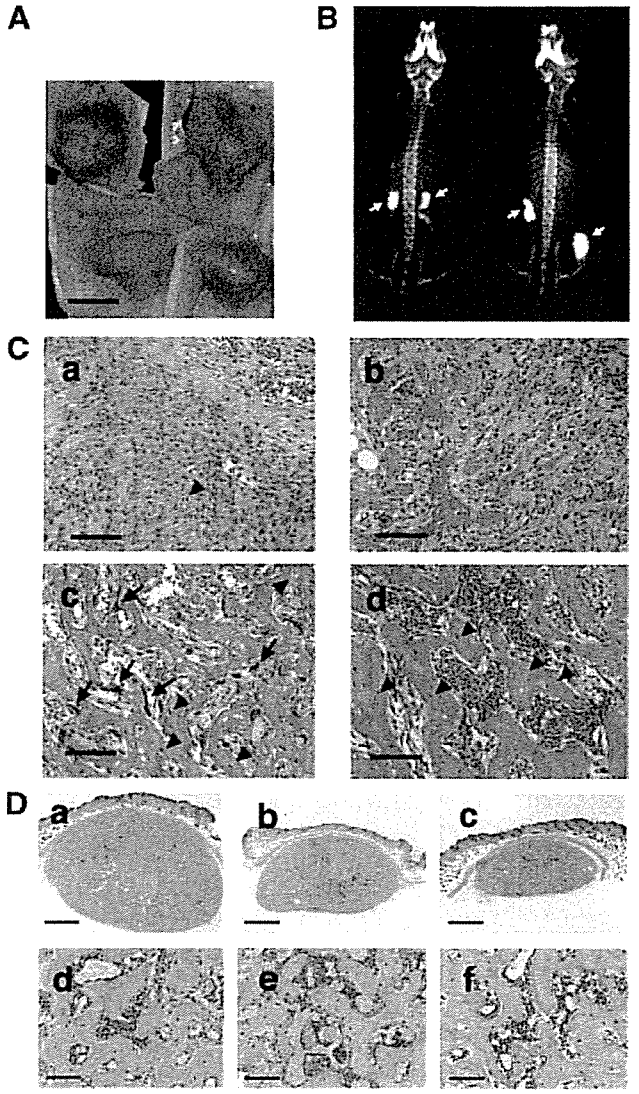

Fig. 1. Time course analysis of hematopoietic induction by KUSA-A1-induced membranous osteogenesis. KUSA-A1 cells were implanted into the subcutaneous tissue of BALB/c nu/nu mice at a density of 2×10^7 cells/200 μl. **A**: Macroscopic view of bone formation at 5 weeks after KUSA-A1 cell injection. **B**: Soft X-ray image of a bone nodule formed by KUSA-A1 cells 5 weeks after implantation. **C**: Histopathological examination of induction of hematopoiesis and bone formation at 1 (**a**), 2 (**b**), 3 (**c**), and 4 (**d**) weeks after KUSA-A1 cell implantation. The mitotic figure of the implanted cell is indicated by an arrowhead (a). Note that numerous osteoclasts (c, arrows) as well as osteoblasts and osteocytes (c, arrowheads) were detected at 3 weeks after implantation. Mature osteocytes were observed at 4 weeks (d, arrowheads). Hematoxylin and eosin stain. Scale bars: 10 mm (A), 230 μm (**C–F**). **D**: Correlation between the number of cells implanted and the size of the bone nodules. Microscopic view of the KUSA-A1 bone 5 weeks after implantation of 2×10^7 (a, d), 1×10^7 (b, **e**), or 5×10^6 (c, **f**) KUSA-A1 cells into subcutaneous tissue. Hematoxylin and eosin stain. Scale bars: 2 mm (a–c), 250 μm (d), 300 μm (e), 250 μm (f).

Expression of major histocompatibility antigen (MHC) after implantation

Marrow stromal cells have been reported to be immunologically tolerant, probably due to lack of transplantation antigen expression. To determine whether KUSA-A1 cells are tolerant when implanted into an allogeneic host, KUSA-A1 cells, which are C3H/He mouse origin, were implanted into BALB/c mice (Fig. 2). Time-course analysis clearly revealed that all of the cells were rejected and formed no bone, but numerous foreign body giant cells were observed (Fig. 2C,D), suggesting that KUSA-A1 cells are immunogenic in our experimental setting.

To determine alterations in MHC antigens after implantation, flow cytometric analysis was performed on KUSA-A1 cells (Fig. 2E, open peaks) and cultured mesenchymal cells obtained from KUSA-A1-induced ectopic bone (Fig. 2E, closed peaks) in BALB/c nu/nu mice. The KUSA-A1 cells started to express one of the MHC antigens, H-2k, after implantation into BALB/c nu/nu mice, but expression of Sca-1 was downregulated. Expression of Lin (CD3, CD4, CD8, B220, Gr-1, Mac-1, and Ter119), c-kit, and CD34 remained unchanged after implantation.

MHC expression of the hematopoietic cells in the KUSA-A1 cell-induced bone

Morphological analysis showed that hematopoiesis took place in the KUSA-A1-induced ectopic bone (Fig. 3A–E). Megakaryocytes (arrows in Fig. 3D), erythrocytes (Fig. 3D,E), and granulocytes (Fig. 3D,E) were detected as well as osteoblasts (arrows in Fig. 3E) and mature osteocytes (arrowheads in Fig. 4E). The hematopoietic cells isolated from the KUSA-A1 cell-induced ectopic bone expressed the H-2d antigen, implying that they were derived from the host cells and had not differentiated from the implanted KUSA-A1 cells.

Cytokine production by the implanted KUSA-A1 cells may not be attributable to the migration of hematopoietic cells

To determine whether cytokines, that is, interleukin-6, macrophage-colony stimulating factor, stem cell factor, fms-like tyrosine kinase-3 ligand, and thrombopoietin, were produced by the implanted cells and contributed to the hematopoiesis, ELISA analysis was performed on the serum from mice with cell implantation as well as conditioned medium of the KUSA-A1 cultures (Fig. 3F). RT-PCR analysis of cytokine gene expression revealed that the KUSA-A1 cells express CSF-1, thrombopoietin, angiotensinogen, c-kit ligand, leptin, lymphotoxin A and B, IL4, IL5, IL6, IL10, IL12B, IL16, IL17B, IL19, and angiopoietin1 genes (Supplementary Figure 1S) and transcriptome analysis revealed that KUSA-A1 cells express the SDF-1 gene at a high level (a frequency of 1.1×10^{-3}) (Sharov et al., 2003). However, none of the cytokine levels increased in the serum.

Analysis of KSL cells in the femur and the ectopic bone, and CFU-S in the peripheral blood and the ectopic bone

To investigate whether HSCs as well as mature hematopoietic cells migrates into the ectopic bone, the proportion of KSL cells was examined. The proportion was found to be the same, that is, 0.08%, in both the host femur (Fig. 4A) and the KUSA-A1 ectopic bone (Fig. 4B), suggesting that the ectopic bone as well as native bone serves microenvironment for HSCs.

The number of CFU-S were also counted in the host femur, peripheral blood, and KUSA-A1-induced bone marrow (Fig. 4C–E), and were found to account for $11.2 \pm 0.8/1.0 \times 10^5$ the cells in the KUSA-A1-induced ectopic bone (Fig. 4E, right). By day 12 the CFU-S of the host femur had increased from 28.3 ± 6.0 to $35.0 \pm 3.4/10^5$ cells (Fig. 4E, left). At day 12 CFU-S were also detected in the peripheral blood from the mice and

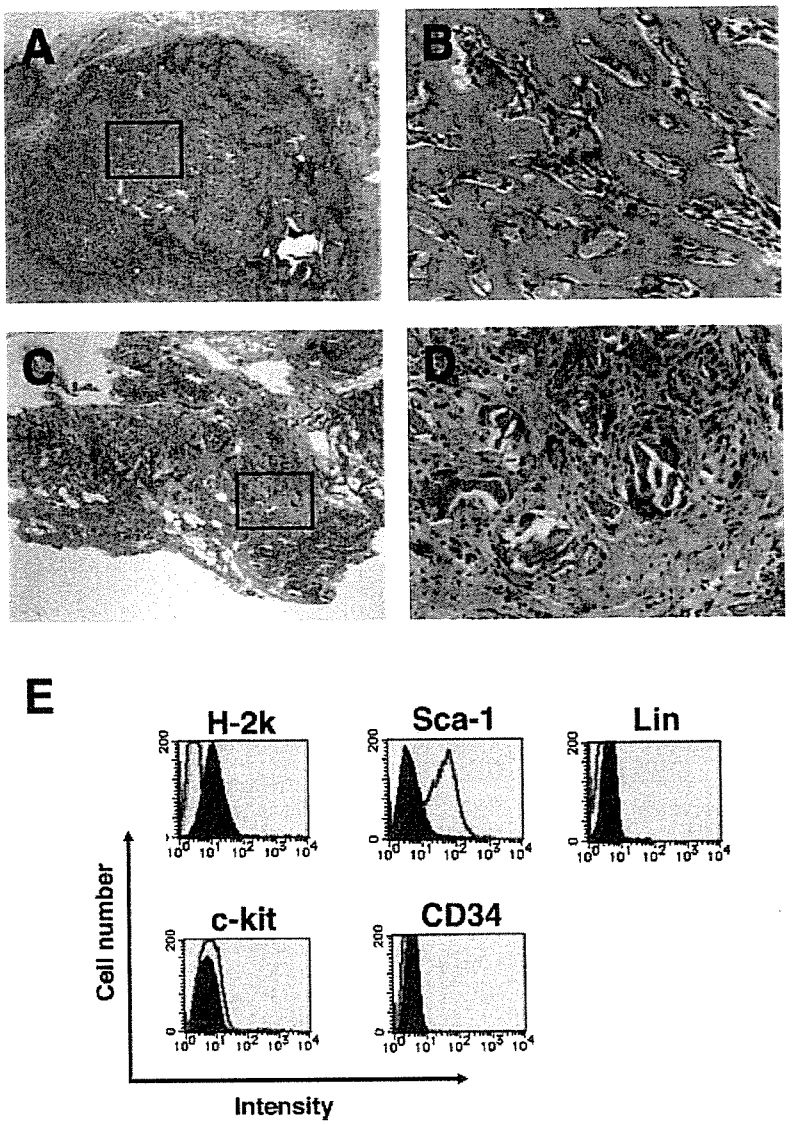

Fig. 2. Rejection of the implanted KUSA-A1 cells in an allogeneic combination. Microscopic view of the generated bone 18 days after the implantation of 5×10^6 KUSA-A1 cells, which were derived from C3H/He mice, into the subcutaneous tissue of syngeneic C3H/He mice (**A, B**) or allogeneic BALB/c mice (**C, D**). Hematoxylin and eosin stain. Parts B and D are higher magnifications of A and C, respectively. **E**: Alterations in cell surface antigens after implantation. Flow cytometric analysis was performed on KUSA-A1 cells (open peaks) and cultured mesenchymal cells obtained from KUSA-A1 ectopic bone (closed peaks) in BALB/c nu/nu mice. The mesenchymal cells were obtained from the KUSA-A1 ectopic bone, and analyzed by flow cytometry. One of major histocompatibility antigens, H-2k, was upregulated, and Sca-1 antigen was downregulated.

accounted for $7.0 \pm 1.7/10^6$ cells (Fig. 4E, middle). In contrast, no CFU-S was detected in the peripheral blood from the mice without KUSA-A1 cell implantation.

Since the upregulation of HSCs in the femurs from the KUSA-A1 cell-implanted mice was rather surprising to us, the time-course of the KSL cell numbers in the femurs from the mice with KUSA-A1 ectopic bone was investigated (Fig. 4F). The number of KSL cells started to increase at 3 weeks, continued to increase to 0.47% by 5 weeks, returned to the basal level, that is, 0.08% at 6 weeks, and then fell down to 0.07% at 7 weeks, implying that the HSC number is strongly correlated with the process of dynamic membranous osteogenesis at the implanted site.

DISCUSSION

Bone remodeling occurs continuously throughout life, and HSCs may mobilize during this remodeling process. The finding in this study support such hypothesis that a very specific niche may be functionally enhanced by bone remodeling (Watt and Hogan, 2000), while a stable or static microenvironment does not support hematopoietic mobilization. For example, accelerated bone remodeling by physical exercise and Vitamin D intake trigger increasing mobilization of HSCs. On the other hand, lack of dynamic bone remodeling in bedridden elderly, astronauts, dieters, postmenopausal women, and patients immobilized for long periods results in downregulation of HSCs in bone marrow.

Upregulation of HSCs by "dynamic" membranous ossification of implanted KUSA-A1 osteoblasts

The cell implantation-based strategy employed in this study revealed that increased niche size following subcutaneous implantation of an osteoblast cell line in syngeneic or immunodeficient mice resulted in

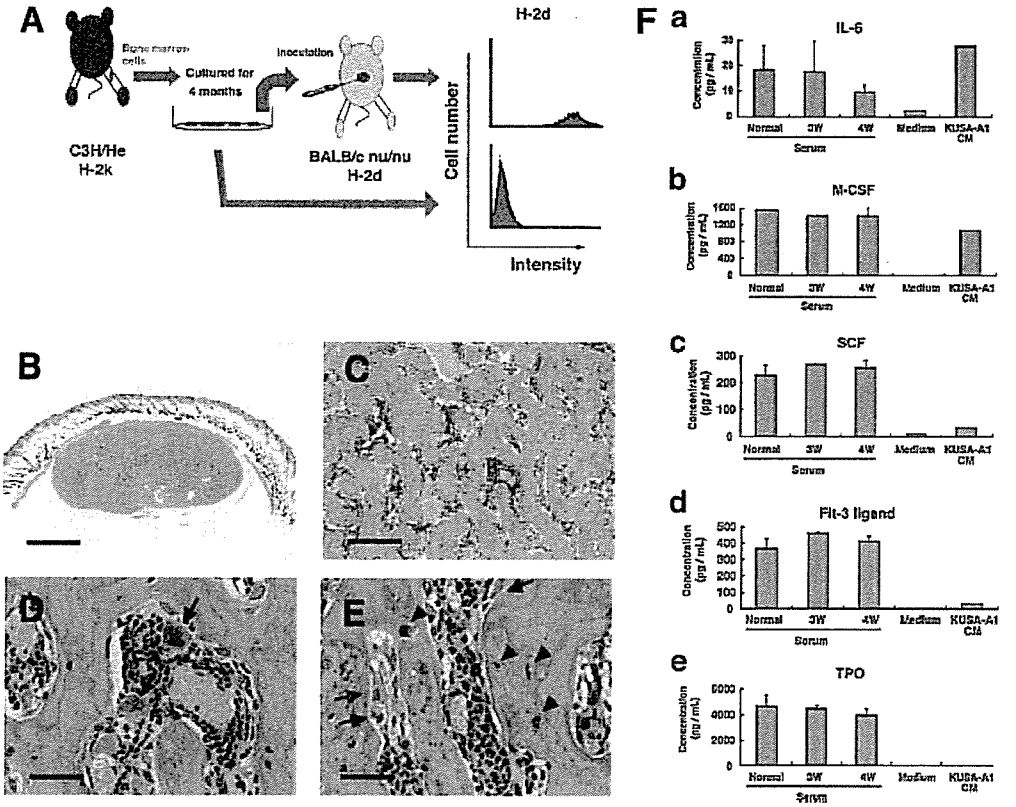

Fig. 3. Hematopoietic cells of host origin in the ectopic bone and serum levels of cytokines after subcutaneous implantation of KUSA-A1 cells. **A**: Flow cytometric analysis of the H-2d antigen in the hematopoietic cells of ectopic bone and KUSA-A1 cells in vitro. The hematopoietic cells in KUSA-A1 bone were examined for expression of the H-2d antigen of the host mice. **B–E**: Histopathological appearance of the hematopoietic cells used for flow cytometric analysis. Trilineage cells, that is, megakaryocytes (D, arrows), erythroblasts (D, E), and granulocytes (E), were observed. Osteoblasts and mature osteocytes are indicated by arrows and arrowheads, respectively (E). Scale bars: 2 mm (B), 400 μm (C), 100 μm (D, E). **F**: Serum levels of interleukin-6 (IL-6) (**a**), macrophage-colony stimulating factor (M-CSF) (**b**), stem cell factor (SCF) (**c**), fms-like tyrosine kinase-3 (Flt-3) ligand (**d**), and thrombopoietin (TPO) (**e**), measured by the ELISA method. The blood samples were obtained at 5 weeks after implantation.

increases in the HSC population. In the HSC population, both the CFU-S and KSL cells increased. The niche that regulates the generation and differentiation of the HSCs was formed following KUSA-A1 cell implantation, and subsequent membranous ossification in vivo. The enlarged area of niche, that is, the inner surface of bone during the dynamic process of membranous osteogenesis may account for the dramatic upregulation of HSCs in the host bone marrow. Once the osteogenic process is terminated, the number of osteoclasts decreases and no bone is remodeled. Furthermore, the number of the KSL cells returns to the basal level in host bone marrow. These facts suggest a correlation between the osteogenic process (Fig. 1C) and increasing number of KSL cells (Fig. 4F).

The source of the CFU-S in the peripheral blood of the mice implanted with KUSA-A1 osteoblasts may be the bone marrow of (a) the ectopic bone; (b) the host femur; (c) both the ectopic bone and the host femur (Fig. 4C). Mobilization of CFU-S from ectopic bone into the peripheral blood is the most likely cause since the induction of HSCs was accompanied by dynamic osteogenesis. The increased HSC number in the host bone marrow can be explained by HSC mobilization from ectopic bone into the peripheral blood. In the normal mice, such migration or mobilization of hematopoietic cells occurs during development. Hematopoietic events in the mouse begin in the yolk sac and aorta-gonad-mesonephros region at day 7 of gestation, and they shift the site to the fetal liver at mid-gestation followed by the bone marrow shortly before birth. The prevailing notion has been that this sequence reflects the migration of HSCs from the yolk sac to the definitive hematopoietic sites. Observation in this study, that is, the generation of ectopic bone in the subcutaneous tissues and the resultant migration of HSCs via the peripheral blood, seems to mimic above process during developments (Dzierzak et al., 1998).

Unexpected upregulation of MHC antigen after implantation of donor cells

Although most HSCs have been reported to express MHCs, that is, HLA in humans, and H-2 antigens in mice, no mesenchymal stem cells have been reported to express MHC antigens at least in vitro (Jiang et al., 2002). Since lack of these antigens on the cell surface may contribute to the induction of tolerance in these cells when transplanted in allogeneic combination, the complete rejection of the transplanted mesenchymal cells and de novo expression of the H-2 antigen after in vivo implantation was contrary to our expectation. We do not know the molecular mechanisms responsible for upregulated expression of H-2 and downregulated expression of Sca-1 after cell implantation, but care should be exercised when mesenchymal cells are implanted for therapeutic purposes, because membrane-bound molecules, including functionally essential molecules, might be modulated after implantation.

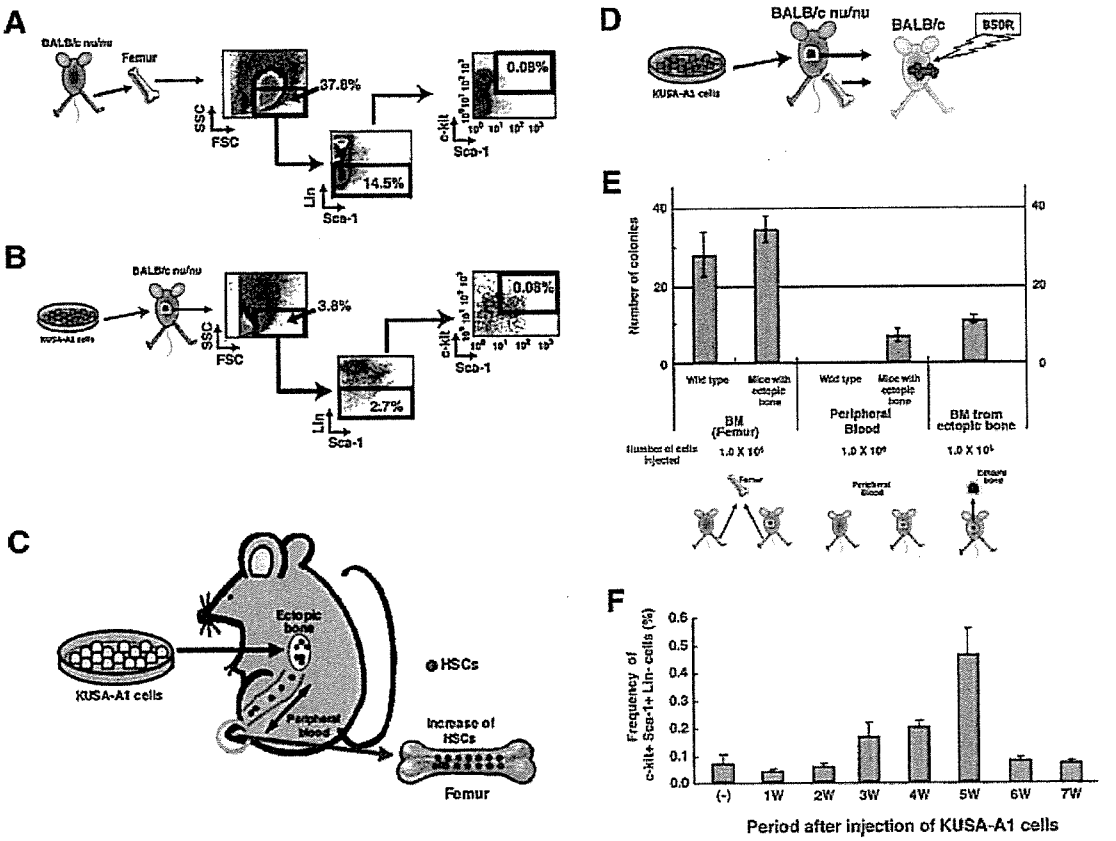

Fig. 4. Mobilization of c-kit$^+$ Sca-1$^+$ Lin$^-$ (KSL) cells in the ectopic bones generated by KUSA-A1 cells. **A** and **B**: Flow cytometric analysis of hematopoietic stem cell markers was performed on hematopoietic cells in the femur of BALB/c nu/nu mice (A) and the ectopic bone generated in BALB/c nu/nu mice (B). KSL cells accounted for 0.08% of the hematopoietic cells in KUSA-A1 bone. **C**: Proposed mechanism of HSC mobilization in the peripheral blood of mice with the ectopic bone, and the increased HSCs in the femur of mice implanted with osteoblasts. Osteoblastic cells whose number has been increased by local injection into the tissues support an increase in number of HSCs in both bone marrow and peripheral blood, as a result of an increase in size of the microenvironment or niche in vivo. The niche size defined by dynamic osteogenic process affects the number of stem cells. **D**: Experimental design to investigate mobilization of CFU-S in the peripheral blood of mice with the ectopic bone, and the proportion of KSL cells in the femur of mice implanted with KUSA-A1 cells. Hematopoiesis was induced in the ectopic bone by KUSA-A1 cell implantation (See Fig. 3). The hematopoietic cells in the ectopic bone and the host femur were analyzed for further CFU-S analysis in mice exposed to 850 cGy irradiation. **E**: CFU-S assay in the marrow cells of the femur of mice not implanted with any cells; the femoral marrow cells of mice with ectopic bone; peripheral blood cells of mice not implanted with cells; peripheral blood cells of mice with ectopic bone; marrow cells in ectopic bone. The blood samples were obtained at 5 weeks after implantation. The number of HSC or CFU-s increased to $11.2 \pm 0.8/1.0 \times 10^5$ cells in the KUSA-A1-induced ectopic bone. CFU-s in the peripheral blood increased to $7.0 \pm 1.7/10^6$ cells at day 12 after implantation of the KUSA-A1 cells while no CFU-s were detected in the peripheral blood from mice without cell implantation. **F**: Time course of the proportion of KLS cells in the femur of mice implanted with KUSA-A1 cells.

Crucial role of marrow stromal subsets in HSC regulation

HSCs are a subset of bone marrow cells that are capable of self-renewal and of forming all types of blood cells. The increases in bone size generated by the spindle-shaped KUSA-A1 osteoblasts correlated with the increase in the number of HSCs. The osteoblasts and a subpopulation of the HSCs expressed N-cadherin, a cell-surface molecule that helps cells adhere to one another, and N-cadherin and -catenin may form important components of the interaction between HSCs and their niche (Zhang et al., 2003). The Notch signaling pathway is also known to regulate cell-fate decisions in many organisms (Calvi et al., 2003). Involvement of cytokine signaling in HSC regulation has been reported to be crucial to the development of blood-forming tissue in embryos. The doubling of bone size mirrored the increase in the HSC population in the mice implanted with KUSA-A1 cells.

The strategy to increase the size of the HSC population by implanting osteoblasts into the subcutaneous tissue to increase the osteoblast cell population may be proven to be of certain clinical value in the future. The concept that a microenvironment or niche controls HSCs may be useful for HSC expansion in vivo, and has potential implications for HSC harvesting and recovery after transplantation (Fig. 4C). Direct implantation of KUSA-A1 cells into syngeneic or immunodeficient mice, in order to better understand the interactions between HSCs and bone marrow, may therefore lead to the development of practical methods of manipulating stem cells and define a model for investigating the impact of the microenvironment on cell physiology (Li et al., 2000). Cellular and molecular identification using the strategy of niche-constituent cells or signaling pathways will provide pharmacological targets with therapeutic potential for stem-cell-based therapies.

ACKNOWLEDGMENTS

This study was supported by a grant from the Ministry of Education, Culture, Sports, Science, and Technology (MEXT) of Japan and the Health and Labour Sciences Research Grants, and the Pharmaceuticals and Medical

Devices Agency to A. U. We thank T. Tsurumi and T. Shimizu for their excellent technical assistance in animal and cell culture.

LITERATURE CITED

Calvi LM, Adams GB, Weibrecht KW, Weber JM, Olson DP, Knight MC, Martin RP, Schipani E, Divieti P, Bringhurst FR, Milner LA, Kronenberg HM, Scadden DT. 2003. Osteoblastic cells regulate the haematopoietic stem cell niche. Nature 425:841–846.

Dzierzak E, Medvinsky A, de Bruijn M. 1998. Qualitative and quantitative aspects of haematopoietic cell development in the mammalian embryo. Immunol Today 19:228–236.

Goodell MA, Brose K, Paradis G, Conner AS, Mulligan RC. 1996. Isolation and functional properties of murine hematopoietic stem cells that are replicating in vivo. J Exp Med 183:1797–1806.

Harrison DE, Russell ES. 1972. The response of W-W v and Sl-Sl d anaemic mice to haemopoietic stimuli. Br J Haematol 22:155–168.

Ikehara S. 2000. Pluripotent hemopoietic stem cells in mice and humans. Proc Soc Exp Biol Med 223:149–155.

Jiang Y, Jahagirdar BN, Reinhardt RL, Schwartz RE, Keene CD, Ortiz-Gonzalez XR, Reyes M, Lenvik T, Lund T, Blackstad M, Du J, Aldrich S, Lisberg A, Low WC, Largaespada DA, Verfaillie CM. 2002. Pluripotency of mesenchymal stem cells derived from adult marrow. Nature 418:41–49.

Kohyama J, Abe H, Shimazaki T, Koizumi A, Nakashima K, Gojo S, Taga T, Okano H, Hata J, Umezawa A. 2001. Brain from bone: Efficient "meta-differentiation" of marrow stroma-derived mature osteoblasts to neurons with Noggin or a demethylating agent. Differentiation 68:235–244.

Li Y, Hisha H, Inaba M, Lian Z, Yu C, Kawamura M, Yamamoto Y, Nishio N, Toki J, Fan H, Ikehara S. 2000. Evidence for migration of donor bone marrow stromal cells into recipient thymus after bone marrow transplantation plus bone grafts: A role of stromal cells in positive selection. Exp Hematol 28:950–960.

Lord BI. 1990. The architecture of bone marrow cell populations. Int J Cell Cloning 8:317–331.

Makino S, Fukuda K, Miyoshi S, Konishi F, Kodama H, Pan J, Sano M, Takahashi T, Hori S, Abe H, Hata J, Umezawa A, Ogawa S. 1999. Cardiomyocytes can be generated from marrow stromal cells in vitro. J Clin Invest 103:697–705.

Matsuzaki Y, Kinjo K, Mulligan RC, Okano H. 2004. Unexpectedly efficient homing capacity of purified murine hematopoietic stem cells. Immunity 20: 87–93.

Mori T, Kiyono T, Imabayashi H, Takeda Y, Tsuchiya K, Miyoshi S, Makino H, Matsumoto K, Saito H, Ogawa S, Sakamoto M, Hata J-I, Umezawa A. 2005. Combination of hTERT and Bmi-1, E6 or E7 induce prolongation of the life span of bone marrow stromal cells from an elderly donor without affecting their neurogenic potential. Mol Cell Biol 25:5183–5195.

Okada S, Nakauchi H, Nagayoshi K, Nishikawa S, Miura Y, Suda T. 1991. Enrichment and characterization of murine hematopoietic stem cells that express c-kit molecule. Blood 78:1706–1712.

Okada S, Nakauchi H, Nagayoshi K, Nishikawa S, Miura Y, Suda T. 1992. In vivo and in vitro stem cell function of c-kit- and Sca-1-positive murine hematopoietic cells. Blood 80:3044–3050.

Osawa M, Hanada K, Hamada H, Nakauchi H. 1996. Long-term lymphohematopoietic reconstitution by a single CD34-low/negative hematopoietic stem cell. Science 273:242–245.

Pittenger MF, Mackay AM, Beck SC, Jaiswal RK, Douglas R, Mosca JD, Moorman MA, Simonetti DW, Craig S, Marshak DR. 1999. Multilineage potential of adult human mesenchymal stem cells. Science 284:143–147.

Schöfield R. 1978. The relationship between the spleen colony-forming cell and the haemopoietic stem cell. Blood Cells 4:7–25.

Sharov AA, Piao Y, Matoba R, Dudekula DB, Qian Y, VanBuren V, Falco G, Martin PR, Stagg CA, Bassey UC, Wang Y, Carter MG, Hamatani T, Aiba K, Akutsu H, Sharova L, Tanaka TS, Kimber WL, Yoshikawa T, Jaradat SA, Pantano S, Nagaraja R, Boheler KR, Taub D, Hodes RJ, Longo DL, Schlessinger D, Keller J, Klotz E, Kelsoe G, Umezawa A, Vescovi AL, Rossant J, Kunath T, Hogan BL, Curci A, D'Urso M, Kelso J, Hide W, Ko MS. 2003. Transcriptome analysis of mouse stem cells and early embryos. PLoS Biol 1:E74.

Siminovitch L, McCulloch EA, Till JE. 1963. The distribution of colony-forming cells among spleen colonies. J Cell Physiol 62:327–336.

Spangrude GJ, Heimfeld S, Weissman IL. 1988. Purification and characterization of mouse hematopoietic stem cells. Science 241:58–62.

Takeda Y, Mori T, Imabayashi H, Kiyono T, Gojo S, Miyoshi S, Hida N, Ita M, Segawa K, Ogawa S, Sakamoto M, Nakamura S, Umezawa A. 2004. Can the life span of human marrow stromal cells be prolonged by bmi-1, E6, E7, and/or telomerase without affecting cardiomyogenic differentiation? J Gene Med 6:833–845.

Terai M, Uyama T, Sugiki T, Li XK, Umezawa A, Kiyono T. 2005. Immortalization of human fetal cells: the life span of umbilical cord blood-derived cells can be prolonged without manipulating p16INK4a/RB braking pathway. Mol Biol Cell 16:1491–1499.

Till JE, McCulloch CE. 1961. A direct measurement of the radiation sensitivity of normal mouse bone marrow cells. Radiat Res 14:213–222.

Till JE, McCulloch EA, Siminovitch L. 1964. A stochastic model of stem cell proliferation, based on the growth of spleen colony-forming cells. Proc Natl Acad Sci USA 51:29–36.

Umezawa A, Maruyama T, Segawa K, Shadduck RK, Waheed A, Hata J. 1992. Multipotent marrow stromal cell line is able to induce hematopoiesis in vivo. J Cell Physiol 151:197–205.

Watt FM, Hogan BL. 2000. Out of Eden: Stem cells and their niches. Science 287:1427–1430.

Weissman IL. 2000. Stem cells: Units of development, units of regeneration, and units in evolution. Cell 100:157–168.

Yoshimoto M, Shinohara T, Heike T, Shiota M, Kanatsu-Shinohara M, Nakahata T. 2003. Direct visualization of transplanted hematopoietic cell reconstitution in intact mouse organs indicates the presence of a niche. Exp Hematol 31: 733–740.

Zhang J, Niu C, Ye L, Huang H, He X, Tong WG, Ross J, Haug J, Johnson T, Feng JQ, Harris S, Wiedemann LM, Mishina Y, Li L. 2003. Identification of the haematopoietic stem cell niche and control of the niche size. Nature 425: 836–841.

0013-7227/06/$15.00/0
Printed in U.S.A.

Endocrinology 147(9):4104–4111

doi: 10.1210/en.2006-0162

Differentiation of Adult Stem Cells Derived from Bone Marrow Stroma into Leydig or Adrenocortical Cells

Takashi Yazawa, Tetsuya Mizutani, Kazuya Yamada, Hiroko Kawata, Toshio Sekiguchi, Miki Yoshino, Takashi Kajitani, Zhangfei Shou, Akihiro Umezawa, and Kaoru Miyamoto

Department of Biochemistry (T.Y., T.M., K.Y., H.K., T.S., M.Y., T.K., Z.S., K.M.), Faculty of Medical Sciences, University of Fukui, Fukui 910-1193, Japan; Core Research for Evolutional Science and Technology (T.Y., T.M., K.Y., H.K., T.S., M.Y., T.K., Z.S., K.M.), Japan Science and Technology Agency, Saitama 332-0012, Japan; and National Research Institute for Child Health and Development (A.U.), Tokyo 157-8535, Japan

Adult stem cells from bone marrow, referred to as mesenchymal stem cells or marrow stromal cells (MSCs), are defined as pluripotent cells and have the ability to differentiate into multiple mesodermal cells. In this study, we investigated whether MSCs from rat, mouse, and human are able to differentiate into steroidogenic cells. When transplanted into immature rat testes, adherent marrow-derived cells (including MSCs) were found to be engrafted and differentiate into steroidogenic cells that were indistinguishable from Leydig cells. Isolated murine MSCs transfected with green fluorescence protein driven by the promoter of P450 side-chain cleaving enzyme gene (CYP11A), a steroidogenic cell-specific gene, were used to detect steroidogenic cell production *in vitro*. During *in vitro* differentiation, green fluorescence protein-positive cells, which had characteristics similar to those of Leydig cells, were found. Stable transfection of murine MSCs with a transcription factor, steroidogenic factor-1, followed by treatment with cAMP almost recapitulated the properties of Leydig cells, including the production of testosterone. Transfection of human MSCs with steroidogenic factor-1 also led to their conversion to steroidogenic cells, but they appeared to be glucocorticoid- rather than testosterone-producing cells. These results indicate that MSCs represent a useful source of stem cells for producing steroidogenic cells that may provide basis for their use in cell and gene therapy. (*Endocrinology* 147: 4104–4111, 2006)

STEM CELLS ARE self-renewing elements with the capacity to generate multiple distinct cell lineages. They exist in various tissues, even in adults, and have been isolated from a variety of differentiated tissues, including bone marrow, umbilical blood, brain, and fat (1–6). Among these, bone marrow-derived mesenchymal stem cells (MSCs), also known as marrow stromal cells, are defined as pluripotent cells and have been shown to differentiate into adipocytes, chondrocytes, osteoblasts, and hematopoietic-supporting stroma both *in vivo* and *ex vivo* (1–3). Furthermore, they are able to generate cells of all three germ layers (7, 8). In addition to their multipotency for differentiation, MSCs have attracted considerable interest for use in cell and gene therapy because these cells can easily be obtained from adult marrow tissue (8–10).

The gonad and adrenal gland are the primary steroidogenic organs in mammals. In the gonad, male Leydig cells or female granulosa and theca cells are responsible for the production of androgens and estrogens. The adrenal cortex produces glucocorticoids and mineralocorticoids, although some androgens are also produced in many species, except rodents. These steroidogenic organs develop from the common adrenogenital primodium, which originates from the intermediate mesoderm (11). Fetal-type steroidogenic cells appear when the adrenogenital primodium differentiates into the adrenal cortex and the gonads of the two sexes. These are replaced by adult-type steroidogenic cells during the period between birth and puberty (12, 13), but these processes are poorly understood.

One approach to resolving the complexities of organogenesis is to use stem cells as a model system for differentiation. In this study, the differentiation of MSCs into steroidogenic cells was examined *in vivo* and *in vitro* by several methods. A number of studies have reported that the injection of MSCs into some tissues leads to the differentiation of the injected cells into tissue-specific cells, probably due to the microenvironment near the injection sites. To determine whether MSCs are able to differentiate into steroidogenic cells, we injected a purified population of rat MSCs into the prepubertal rat testis and examined the fate of these cells by immunohistochemistry. In addition, the spontaneous differentiation of MSCs to specific cells can be monitored by the expression of specific genes in the differentiated cells. One such experimental approach, known as a promoter-sorting method, is to use fluorescence-activated cell sorting (FACS) to select green fluorescence protein (GFP)-positive MSCs in which the expression of GFP is under the control of the promoter of a gene that is expressed in a cell type-specific fashion. In this study, to demonstrate the emergence of steroidogenic cells from isolated MSCs *in vitro*, a GFP expression vector driven by the CYP11A promoter (CYP11A is a

First Published Online May 25, 2006

Abbreviations: ES, Embryonic stem; FACS, fluorescence activated cell sorting; GFP, green fluorescence protein; hMSC, human MSC; 3β-HSD I, 3β-hydroxysteroid dehydrogenase I; 17β-HSD III, 17β-hydroxysteroid dehydrogenase III; mMSC, murine MSC; MSC, mesenchymal stem cell; P450arom, cytochrome P450 aromatase; P450c17, cytochrome P450 17α-hydroxylase; P450c21, cytochrome P450 steroid 21-hydroxylase; P450scc, P450 side-chain cleaving enzyme; SF, steroidogenic factor; StAR, steroidogenic acute regulatory protein.

Endocrinology is published monthly by The Endocrine Society (http://www.endo-society.org), the foremost professional society serving the endocrine community.